

This is to certify that the

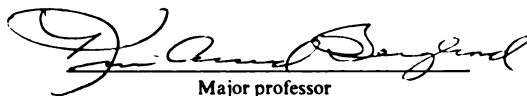
dissertation entitled

Synthesis and Characterization of Tailor-Made
Additives for Inhibition of Sparingly Soluble
Calcium Salt Crystallization
presented by

Charles O. Ngowe

has been accepted towards fulfillment
of the requirements for

Ph.D. degree in Chemistry



Major professor

Date 12 DEC 2002

**Synthesis and Characterization of Tailor-Made Additives for Inhibition
of Sparingly Soluble Calcium Salt Crystallization**

By

CHARLES OWINO NGOWE

A DISSERTATION

Submitted to
Michigan State University
in partial fulfillment of the requirements
for the degree of

DOCTOR OF PHILOSOPHY

Department of Chemistry

2002

ABSTRACT

SYNTHESIS AND CHARACTERIZATION OF TAILOR-MADE ADDITIVES FOR INHIBITION OF SPARINGLY SOLUBLE CALCIUM SALT CRYSTALLIZATION

By

CHARLES OWINO NGOWE

Tailor-made additives were designed and used to modify the nucleation and growth kinetics of calcium oxalate crystallizing from aqueous solution. Tailor-made inhibitors can be used for a variety of purposes that include crystal morphology engineering, kinetic resolution of racemates, reduction of crystal symmetry, assignment of absolute configuration of chiral molecules and polar crystals and control of crystal polymorphism. The molecules of the present study influenced both the morphology and phase transformation of calcium oxalate crystals.

Calcium oxalate, CaC_2O_4 , is a sparingly soluble salt widely found in nature. Three hydrate forms of the salt are known including the monohydrate, the dihydrate, and the trihydrate. In the pulp and paper industries, CaC_2O_4 is notorious for forming scale deposits on the equipment. In animals, CaC_2O_4 occurs as a crystal in the urinary tract and

constitutes the largest composition in kidney and bladder stones. Clinical management of kidney stones includes taking citric acid supplements which are inhibitors of calcium salt crystallization; however, the amount of citric acid that must be consumed is relatively large (in excess of 2-8 grams per day). Coincidentally, large amounts of amino acids (0.8%) are found in kidney stone matrix, and they too have long been considered as crystallization inhibitors; however, several studies have proven otherwise. To improve efficacy of amino acids in this application, we have derivatized several amino acids with cis-exoxysuccinic acid. Subsequently, the crystallization of calcium oxalates in the presence of the derivatized amino acids was studied at ambient temperature. The glycine and the glutamic derivative selectively inhibited the phase transformation and stabilized the dihydrate form of calcium oxalate, while others allowed phase transformation to take place from a metastable calcium oxalate trihydrate, COT, to the thermodynamically stable monohydrate, COM. The lysine derivative inhibited the nucleation and the crystal growth of calcium oxalate much better than citric acid although they both had very little effect on CaC_2O_4 phase transformation. In all cases, the additives modified the crystal shape of the dihydrate form of calcium oxalate.

DEDICATION

To Joseph Omony, Adhadha Athieno
And Jason and Lucy Greer

ACKNOWLEDGMENTS

I will always be indebted to my advisor Prof. Kris Berglund for making this possible. He allowed me the freedom to develop as an intellectual at my own pace, and gave me much needed advise at critical junctions in my academic career. I can always count on him giving me his honest opinion about any subject. One of the greatest things I learned from Kris is keeping my mind focused. Thank you for helping me cross this bridge.

My wife Karen Ngowe aka Lady Love Karen (LLK) deserves many thanks for believing in me and pushing me beyond my own limits. Without her moral and emotional support I could not have done this alone. Thank you for all your encouragements and being the strength our family that we depend on. I love you a billion times plus one.

To my children Athieno Lironah Ngowe named after my last surviving grandmother, and Yosef Opoya Ngowe named after the family that raised my great grandfather, I extend many thanks in your honor. Only hard work and perseverance will guarantee you any success in life. Never give up on anything and always believe in yourself. The extra energy and motivation I needed to complete my academic career was driven by the love for you both.

My poor mother Dalia Owino, thank you for giving me all the extra help I needed in order to perform well in school. My siblings always accused you for loving me more but I believe that you loved us all the same. However, I needed your nurturing the most. This historical achievement is in your honor.

I cannot forget my father Owino Wodomony, and my in-laws Barry and Judy Kanne. Thank you for investing so much of your time and finances on my education. I

would have had greater difficulty in achieving this goal without your presence in my life. Thank you for everything.

Also thanks to my second advisor Prof. Gary Blanchard for all his guidance and acceptance in his group as one of his own. Thanks to the many advises that you gave me, and for listening to all my problems. To the rest of my committee members, Prof. Malezcka and Prof. Bohran, I enjoyed the support you afforded me.

Last, but not least is those that most certainly need to be thanked are Dr Stephen Bakiamoh and Dr. Jaycoda Major for all the late nights we spent coaching, supporting, and teaching one another. Dr. Dilum Dunuwila, thanks for all the discussions about crystallization as well as listening to all my problems. I will always depend on your support. The rest of the labmates past and present; Parminder, Sri, Mike, Adam, Carinna, Fang, Al, Anna, Lilli, Javier, DeeDee, Johnny, Matt, Rosanna, and Hasan, thanks for all your support.

TABLE OF CONTENTS

List of Tables.....	ix
List of Figures.....	x
List of Schemes.....	xiv
List of Spectra.....	xv
List of Abbreviations.....	xvi
Introduction	
Chapter 1	
BACKGROUND AND LITERATURE REVIEW	
1.1 Calcium oxalate crystal growth in kidney tones	1
1.1.1 The Supersaturation/ Crystallization Theory of Kidney Stone Formation.....	4
1.1.2 The Matrix Theory of Kidney Stone Formation.....	5
1.1.3 The Promoter/Inhibitor Theory of Kidney Stone Formation.....	6
1.2 Calcium Oxalate Crystal Growth in Plants.....	7
1.2.1 Environmental and Economical Impact of Calcium Oxalate deposits.....	8
1.2.2 Calcium Oxalate as a Sparingly Soluble Salt.....	9
1.3 Crystallization Kinetics	11
1.3.1 Supersaturation	13
1.3.2 Homogeneous Nucleation	14
1.3.3 Heterogeneous Nucleation	15
1.3.4 Crystal Growth Theory	16
1.3.4.1 Burton, Cabrera, and Frank Model	17
1.3.4.2 Birth and Spread Model	20
1.3.4.3 Diffusion-controlled growth	22
1.3.5 Crystal Shape	24
1.3.6 Crystal Habit Modification	29

1.3.7 Phase Transformation.....	32
1.4 References	34
Chapter 2	
SYNTHESIS of SIMPLE ORGANIC CHELATES DERIVED FROM AMINO ACID AND EPOXYSUCCINIC ACID FOR INHIBITION OF CALCIUM OXALATE CRYSTALGROWTH.....	38
2.1 Background	39
2.2 Experimental	41
2.2.1 Calibration curve	47
2.2.2 Titration.	47
2.2.3 Nephelometry experiment	48
2.3 Results and Discussion	51
2.3.1 Chelation constants	51
2.3.2 Crystallization kinetics	56
2.4 Conclusions	61
2.5 References	62
Chapter 3	
THE INFLUENCE OF TAILOR-MADE IMPURITIES OF AMINOACID DERIVATIVES ON THE MORPHOLOGY AND PHASE TRANSFORMATION OF CALCIUM OXALATE HYDRATES.....	64
3.1 Background	66
3.2 Experimental	68
3.3 Results and Discussion	69
3.4 Conclusion	91
3.5 References	92
Chapter 4	
FUTURE STUDIES	
4.1 Introduction	95
4.2 Proposed Studies	96
4.2.1 Constant composition method	96
4.2.2 Synthesis of amino acid derivatives	98
4.3 References	99
Conclusion	100

LIST OF TABLES

Table 1.1	Common precipitates in kidney stone disease	2
Table 2.1	Calcium chelation capacity of amino acid derivatives compared to citrate as determined by calcium-selective electrode (model 97-20 ionplus electrode).	61
Table 2.2	Effects of inhibitors on calcium oxalate polymorph nucleation and crystal growth. Experimental conditions: calcium oxalate, and inhibitor concentrations were all at 0.8 mM, T°, 28.0°C; pH 5.5; ionic strength, 0.15M.	66

LIST OF FIGURES

Figure 1.1	Flow chart depicting the different types of nucleation and the corresponding subcategories.	12
Figure 1.2	Development of a growth spiral starting from a screw dislocation (a) to spiral staircase (c).	18
Figure 1.3	Depicts such a polycrystalline growth by the birth and spread (B+S) mechanism.	21
Figure 1.4	Equilibrium crystal shape as described by Wulff's theorem. In this case $\gamma_1 < \gamma_2$	25
Figure 1.5	Hypothetical three-dimensional crystal presenting the three main types of possible faces: flat (F), step (S) and kink (K) faces.	27
Figure 1.6	Influence of impurity adsorption on the crystal habit, for the case of adipic acid.	30
Figure 1.7	Typical solubility profiles and pertinent supersaturation values.	33
Figure 2.1	Optical schematic of the spectrometer for nephelometry study.	56
Figure 2.2	A plot of moles of bound Ca^{2+} vs moles of titrant (lysine derivative). Data of bound calcium was from the average of three replicates. Experimental conditions: 200 ppm calcium concentration, 0.03M $\text{NH}_4\text{Cl}/0.07\text{M}$ NH_4OH buffer (pH=9.5, ionic strength of 0.1M NaCl, 25 °C).	58
Figure 2.3	pK _{Ca} verses lysine derivative concentration. The pK _{Ca} was determined from the average of three replicates. Experimental conditions: 200 ppm calcium concentration, 0.03M $\text{NH}_4\text{Cl}/0.07\text{M}$ NH_4OH buffer (pH=9.5, ionic strength of 0.1M NaCl, 25 °C).	60

Figure 2.4	Typical curve of calcium oxalate crystallization using nephelometry. Experimental conditions: calcium concentration, 0.8 mM, oxalate concentration, 0.8 mM; T°, 28.0°C; pH 5.5; ionic strength, 0.15M NaCl. The clear line represents the smoothed data using Savitsky-Golay algorithm.	63
Figure 2.5	A typical desupersaturation curve for the system CaCl ₃ ·2H ₂ O + Na ₂ C ₂ O ₄ . Experimental conditions: calcium concentration, 0.8 mM, oxalate concentration, 0.8 mM; T°, 28.0°C; pH 5.5; ionic strength, 0.15M NaCl.	65
Figure 3.1a	Raman spectra of calcium oxalate hydrates after 1 hour in solution. a) alanine derivative, b) glycine derivative, c) arginine derivative, d) citrate, e) glutamic derivative, f) control, g) lysine derivative, h) aspartic derivative. Experimental conditions: calcium concentration, 0.8 mM, oxalate concentration, 0.8 mM; T°, 28.0°C; pH 5.5; ionic strength, 0.15M NaCl. Concentration of additives, 0.8mM.	76
Figure 3.1b	Raman spectra of calcium oxalate hydrates after 24 hours in solution. a) alanine derivative, b) arginine derivative, c) control, d) glutamic derivative, e) glycine derivative, f) citrate, g) lysine derivative, h) aspartic derivative. Experimental conditions: calcium concentration, 0.8 mM, oxalate concentration, 0.8 mM; T°, 28.0°C; pH 5.5; ionic strength, 0.15M NaCl. Concentration of additives, 0.8mM.	77
Figure 3.2	ESEM of a typical COD morphology. Experimental conditions: calcium concentration, 0.8 mM, oxalate concentration, 0.8 mM; T°, 28.0°C; pH 5.5; ionic strength, 0.15M NaCl.	79
Figure 3.3a	ESEM of COD formed in the presence of 0.8 mM glycine derivative after left insolution for 1 hour. Experimental conditions: calcium concentration, 0.8 mM, oxalate concentration, 0.8 mM; T°, 28.0°C; pH 5.5; ionic strength, 0.15M NaCl.	80
Figure 3.3b	ESEM of COD formed in the presence of 0.8 mM β-alanine derivative after left insolution for 1 hour. Experimental conditions: calcium concentration, 0.8 mM, oxalate concentration, 0.8 mM; T°, 28.0°C; pH 5.5; ionic strength, 0.15M NaCl.	81

Figure 3.3c	ESEM of COD formed in the presence of 0.8 mM glutamic derivative after left in solution for 1 hour. Experimental conditions: calcium concentration, 0.8 mM, oxalate concentration, 0.8 mM; T°, 28.0°C; pH 5.5; ionic strength, 0.15M NaCl.	82
Figure 3.3d	ESEM of COD formed in the presence of 0.8 mM arginine derivative after left in solution for 1 hour. Experimental conditions: calcium concentration, 0.8 mM, oxalate concentration, 0.8 mM; T°, 28.0°C; pH 5.5; ionic strength, 0.15M NaCl.	83
Figure 3.4	ESEM of COD formed in the presence of 0.8 mM citrate after left in solution for 1 hour. Experimental conditions: calcium concentration, 0.8 mM, oxalate concentration, 0.8 mM; T°, 28.0°C; pH 5.5; ionic strength, 0.15M NaCl.	84
Figure 3.5	ESEM of COD formed in the presence of 0.8 mM glutamic derivative after left in solution for 24 hours. Experimental conditions: calcium concentration, 0.8 mM, oxalate concentration, 0.8 mM; T°, 28.0°C; pH 5.5; ionic strength, 0.15M NaCl.	85
Figure 3.6	ESEM of COD formed in the presence of 0.8 mM glycine derivative after left in solution for 24 hours. Experimental conditions: calcium concentration, 0.8 mM, oxalate concentration, 0.8 mM; T°, 28.0°C; pH 5.5; ionic strength, 0.15M NaCl.	86
Figure 3.7	ESEM of COD formed in the presence of 0.8 mM alanine derivative after left in solution for 24 hours. Experimental conditions: calcium concentration, 0.8 mM, oxalate concentration, 0.8 mM; T°, 28.0°C; pH 5.5; ionic strength, 0.15M NaCl.	89
Figure 3.8	ESEM of COD formed in the presence of 0.8 mM arginine derivative after left in solution for 24 hours. Experimental conditions: calcium concentration, 0.8 mM, oxalate concentration, 0.8 mM; T°, 28.0°C; pH 5.5; ionic strength, 0.15M NaCl.	90

Figure 3.9a	ESEM of COD formed in the presence of 0.8 mM citrate derivative after left in solution for 24 hours. Experimental conditions: calcium concentration, 0.8 mM, oxalate concentration, 0.8 mM; T°, 28.0°C; pH 5.5; ionic strength, 0.15M NaCl.	91
Figure 3.9b	ESEM of COD formed in the presence of 0.8 mM lysine derivative after left in solution for 24 hours. Experimental conditions: calcium concentration, 0.8 mM, oxalate concentration, 0.8 mM; T°, 28.0°C; pH 5.5; ionic strength, 0.15M NaCl.	92
Figure 3.9c	ESEM of COD formed in the absence of additives after left in solution for 24 hours. Experimental conditions: calcium concentration, 0.8 mM, oxalate concentration, 0.8 mM; T°, 28.0°C; pH 5.5; ionic strength, 0.15M NaCl.	93
Figure 3.9d	ESEM of COD formed in the presence of 0.8 mM aspartic derivative after left in solution for 24 hours. Experimental conditions: calcium concentration, 0.8 mM, oxalate concentration, 0.8 mM; T°, 28.0°C; pH 5.5; ionic strength, 0.15M NaCl.	94
Figure 3.10	XRD spectra of COD crystal of the control sample, and the samples formed in the presence of lysine derivative, and citrate after left in solution for an hour. Experimental conditions: calcium concentration, 0.8 mM, oxalate concentration, 0.8 mM; T°, 28.0°C; pH 5.5; ionic strength, 0.15M NaCl.	95
Figure 3.11	XRD spectra of COD crystal of the control sample, and the samples formed in the presence of additives (glutamic and glycine derivative) which prevented phase transformation of COD crystals after it was left in solution for 24 hours. Experimental conditions: calcium concentration, 0.8 mM, oxalate concentration, 0.8 mM; T°, 28.0°C; pH 5.5; ionic strength, 0.15M NaCl.	96

LIST OF SCHEMES

Scheme 2.1	Synthesis of lysine derivative (6-(1,1-Dicarboxy-2-hydroxy-ethylamino)-2-(1,2-dicarboxy-2-hydroxy-ethylamino)-hexanoic acid).	42
Scheme 2.2	Synthesis of arginine derivative (2-(1-Carboxy-4-guanidino-butylamino)-3-hydroxy-succinic acid).	44
Scheme 2.3	Synthesis of glutamic derivative (2-(1,2-Dicarboxy-ethylamino)-pentanedioic acid).	46
Scheme 2.4	Synthesis of aspartic derivative (2-(1,2-Dicarboxy-ethylamino)-3-hydroxy-succinic acid).	48
Scheme 2.5	Synthesis of glycine derivative (2-(Carboxymethyl-amino)-3-hydroxy-succinic acid).	50
Scheme 2.6	Synthesis of β -alanine derivative (2-(2-Carboxy-ethylamino)-3-hydroxy-succinic acid).	52
Scheme 3.1	Tailor-made additives synthesized by reacting cis-epoxysuccinic acid and amino acid. See chapter 2 for more details on the synthesis procedure.	70

LIST OF SPECTRA

Spectrum 2.1	¹ H-NMR spectrum of lysine derivative (6-(1,1-Dicarboxy-2-hydroxy-ethylamino)-2-(1,2-dicarboxy-2-hydroxy-ethylamino)-hexanoic acid).	41
Spectrum 2.2	¹ H-NMR spectrum of arginine derivative (2-(1-Carboxy-4-guanidino-butylamino)-3-hydroxy-succinic acid).	44
Spectrum 2.3	¹ H-NMR spectrum of glutamic derivative (2-(1,2-Dicarboxy-ethylamino)-pentanedioic acid).	46
Spectrum 2.4	¹ H-NMR spectrum of aspartic derivative (2-(1,2-Dicarboxy-ethylamino)-3-hydroxy-succinic acid).	48
Spectrum 2.5	¹ H-NMR spectrum of glycine derivative (2-(Carboxymethyl-amino)-3-hydroxy-succinic acid).	50
Spectrum 2.6	¹ H-NMR spectrum of β -alanine derivative (2-(2-Carboxy-ethylamino)-3-hydroxy-succinic acid).	52

LIST OF ABBREVIATIONS

A	preexponential factor
κ	Boltzmann's constant
T	temperature
ΔG_0	free energy change for an aggregate undergoing a phase transition
ΔG_v	volume free energy change
ΔG_s	surface free energy change
α	volume-shape factor
r	characteristic length of the crystallizing solute
v	molecular volume of the crystallizing solute
β	area shape factor
γ	interfacial energy per unit area
R	growth rate of a crystal face
A	combination of physical constants of the system including adsorption, surface diffusion, and growth unit incorporation factors
σ	supersaturation
δ	boundary layer thickness
λ	edge free energy per molecule of the nucleus
J_2	the 2D nucleation rate
d	the height of the layer
S	the area of the face
A	surface area of the crystal
D	diffusion coefficient
C	bulk concentration
C_i	interfacial concentrations
k_d	diffusion controlled rate
k_r	solute incorporation rate
k_g	crystal growth rate
η	A quantitative measure of the influence of any resistance to growth
Da	represents the ratio of the pseudo-first-order rate coefficient at the bulk conditions to the mass transfer
ω	the mass fraction of solute in solution
a_2	the activity of the impurity
τ	transformation time
τ_G	growth time
τ_D	dissolution time

Chapter 1

INTRODUCTION

BACKGROUND AND LITERATURE REVIEW

1.1 Calcium Oxalate Crystal Growth in Kidney Stones

The major components of urinary stones are calcium oxalate (CaC_2O_4) and calcium phosphate.¹ Other compounds contributing to the mineral portion of stones and are listed in Table 1.1. Kidney stones are mostly mineral in composition with only about 2.5 percent of the weight of a typical stone due to organic compounds from the urine, known as the stone matrix.² Calcium oxalate monohydrate (COM), dihydrate (COD), and trihydrate (COT) are all found in kidney stones with COM occurring most frequently followed by COD.³ COT occurs least often, and has been reported in only a few cases.^{4,5}

Chemical Name	Mineral Name	Formula
calcium oxalate monohydrate	whewellite	$\text{CaC}_2\text{O}_4 \cdot \text{H}_2\text{O}$
calcium oxalate dihydrate	weddellite	$\text{CaC}_2\text{O}_4 \cdot 2\text{H}_2\text{O}$
calcium oxalate trihydrate		$\text{CaC}_2\text{O}_4 \cdot 3\text{H}_2\text{O}$
basic calcium hydrogen phosphate	hydroxyapatite	$\text{Ca}_5(\text{PO}_4)_3(\text{OH})$
calcium hydrogen phosphate	brushite	$\text{CaHPO}_4 \cdot 2\text{H}_2\text{O}$
tricalcium phosphate	whitlockite	$\text{Ca}_3(\text{PO}_4)_2$
magnesium ammonium phosphate hexahydrate	struvite	$\text{Mg}(\text{NH}_4)(\text{PO}_4) \cdot 6\text{H}_2\text{O}$
uric acid		$\text{C}_5\text{H}_4\text{N}_4\text{O}_3$
uric acid dihydrate		$\text{C}_5\text{H}_4\text{N}_4\text{O}_3 \cdot 2\text{H}_2\text{O}$
monosodium urate monohydrate		$\text{NaC}_5\text{H}_4\text{N}_4\text{O}_3 \cdot \text{H}_2\text{O}$
I-cystine		$\text{S}_2\text{C}_6\text{H}_{12}\text{N}_2\text{O}_4$
octacalcium phosphate		$\text{Ca}_8\text{H}_2(\text{PO}_4)_6 \cdot 5\text{H}_2\text{O}$
magnesium hydrogen phosphate trihydrate	newberite	$\text{MgHPO}_4 \cdot 3\text{H}_2\text{O}$

Table 1.1

Common precipitates in kidney stone disease³

Urinary stone formation theories include supersaturation/crystallization, urinary inhibitors, epitaxy, matrix, and combinations of these processes.^{2,6,7} Urine is a medium unique in its ability to hold solutes (i.e, calcium, oxalate) in solution. In normal urine, the concentration of calcium oxalate salt is four times higher than its solubility in water.⁸ Urinary supersaturation/crystallization is necessary for the formation of stones. As concentrations of solutes increase, the solubility product is reached, above which dissolved salts can form nuclei of its solid phase (the metastable zone). These nuclei can form heterogeneously, that is, on foreign surfaces (other crystals, cellular debris, urinary casts, epithelial lining, etc).⁹ Solute levels reaching the formation product and beyond (the supersaturated zone) may form crystal nuclei homogeneously. Homogenous nucleation occurs in pure solution and requires more thermodynamic energy in order for a stable nuclei to form from which crystal growth can take place. Heterogeneous nucleation is thought to initiate crystal formation. These crystals may attach to the epithelial lining of uriniferous tubules/collecting ducts and subsequently serve as crystal growth sites. Small stones can grow and either spontaneously pass or become large and can lead to obstruction, colic, and/or infection.

Calcium oxalate crystallization from aqueous solution results in the formation of three types of hydrates: the monohydrate, the dihydrate, and the trihydrate, depending on solution conditions, including concentrations of the crystallizing species, the solution temperature, the pH, the ionic strength, and the concentrations of growth-modifiers.¹⁰ These effects include increases or decreases in the following: 1) the numbers of crystals nucleated per solution volume, 2) the time required for the first crystal nuclei to form, or the induction time¹¹, and 3) the rate at which the individual faces of a crystal grow. In

addition, the crystal habit and the crystal phase formed (monohydrate, dihydrate, or trihydrate, in the case of calcium oxalate) also depend on solution conditions.

Subsequent agglomeration (the formation of multi-crystal masses) of growing crystals also depends on the various solution conditions. The effects of several solution parameters on nucleation, growth, and agglomeration have been reviewed by Finlayson.¹²

1.1.1 The Supersaturation/ Crystallization Theory of Kidney Stone Formation

The supersaturation theory of kidney stone formation hypothesizes that calcium oxalate kidney stone formation is wholly due to an increased supersaturation of calcium oxalate in the urine.¹³ This increase is thought to be the result of higher output of calcium and oxalate ions by the kidneys either because of greater ingestion of these substances or through some metabolic malfunction in the body. The high supersaturation of calcium oxalate leads to nucleation of crystals in either free solution or on the luminal walls.

These two modes of nucleation suggest two possible mechanisms for the initiation of stone growth, the free particle mechanism and the fixed particle mechanism.¹² Rapidly growing crystals flowing freely in solution can, after reaching sufficient size, become trapped somewhere in the urinary tract, forming the embryos of a stone. According to the free particle theory, other crystals and urinary debris collide with the entrapped crystal and stick to it, and the stone continues to grow in this manner. In the fixed particle mechanism, a crystal nucleates on a luminal wall grows and attracts urinary debris. Accumulation of organic and mineral matter gradually leads to stone formation. Alternatively, the crystals may agglomerate together freely in the urine solution forming a multi-crystal mass which becomes too large to pass. The agglomerate then acts as a nidus for stone growth in much the same way as a single crystal.

The supersaturation levels of both stone-forming and non-stone-forming urines are high enough for crystals to form,¹⁴ yet crystals occasionally lead to stone formation in the former while they pass harmlessly from the latter. Even though stone-forming urines often show a greater volume of crystals than that observed in non-stone-forming urine¹⁵, at the supersaturation level commonly observed for stone-forming urine, calcium oxalate growth rates are not fast enough to cause blockage of the urinary tract solely due to crystal growth. Therefore, the hyperexcretion/supersaturation theory does not fully explain stone formation. This theory simply suggests one causative factor in the disease solution conditions conducive to rapid crystal nucleation and growth. The other two theories, the matrix theory and the promoter/inhibitor theory, attempt to explain how crystal nucleation, growth, and agglomeration are affected by solution conditions other than supersaturation.

1.1.2 The Matrix Theory of Kidney Stone Formation

The matrix theory of kidney stone formation hypothesizes that the nucleation of calcium oxalate crystals is promoted by the existence of a mucous organic matrix deposited in the urinary tract.^{16,17} This matrix is composed of various organic macromolecules such as glycosaminoglycans and glycoproteins that are thought to precipitate from urine. As they precipitate, they form a loose mucous mass in the tract. This mucous matrix serves as a substrate for crystal nucleation. Crystal nuclei form over the matrix and subsequently grow, causing encrustation and hardening of the forming kidney stone. The tendency for deposition of the matrix is thought to be one factor that separates stone-formers from non-stone-formers and is thought to be a function of the excretion of macromolecules into the urine from various sources in the body.

The matrix theory lacks credibility in that there is a lack of evidence supporting the idea of large-scale deposition of the organic macromolecules prior to encrustation. A more plausible explanation, and one that seems to be more verifiable, is the promoter/inhibitor theory.

1.1.3 The Promoter/Inhibitor Theory of Kidney Stone Formation

The promoter/inhibitor theory of kidney stone formation is based on the tendency for calcium oxalate crystals to nucleate and grow in urine at a higher rate for stone-formers than for non-stone formers.¹⁸ This is not, however, necessarily due to a greater calcium oxalate supersaturation in stone-forming urine, as noted above. Rather, there are certain chemical species in urine that modify the nucleation, growth, and/or agglomeration of calcium oxalate.

Various substances have been implicated as growth modifiers, including macromolecular species such as glycosaminoglycans and glycoproteins. The modification may be inhibitory or promotional depending on the substance present, the amount present, and the process being considered. Normal urine contains macromolecules that inhibit crystal growth but promote the nucleation of crystals.¹⁹ There is apparently a greater concentration of these macromolecules in normal urine than in stone-forming urine.²⁰ The creation of many small, slowly growing crystals in normal urine allows excretion before stone formation can occur. Urinary macromolecules may also inhibit the agglomeration of crystals.²¹ Enhancement of nucleation by urinary macromolecules and the apparent increase in the probability of agglomeration due to a higher concentration of crystals in urine is offset by the inhibition of agglomeration by urinary macromolecules. Thus, the promoting effect of certain urinary macromolecules

on crystal nucleation is offset by their inhibitory effect on crystal growth and agglomeration. The net effect is that crystals pass from the urinary tract before stone formation can occur. The low concentration or lack of these macromolecules in stone-forming urine is one possible cause of an increased tendency to form kidney stones.

The promoter/inhibitor theory is actually an extension of supersaturation theory in that high levels of calcium oxalate supersaturation are still required to form crystals and consequent stones. The overall mechanism of stone formation, whether by a fixed or free particle mechanism, is still a matter for debate and can only be resolved by experiments simulating the complete environment of the kidney, including the flow characteristics, luminal walls, and insoluble debris. The plausibility of the theory can be and has been tested by simple experiments of solution crystallization in the presence of various modifiers. Experiments such as these, while intended to explain kidney stone formation, also contribute to the general understanding of crystal growth.

1.2 Calcium Oxalate Crystal Growth in Plants

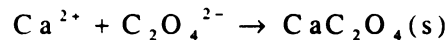
A vast array of organisms produce biological minerals, or “biominerals.” Biominerals encompass a wide spectrum of scale and composition, from macroscopic structures such as vertebrate bone, composed of apatite, to microscopic silicon frustules of diatoms and subcellular ferrimagnetic particles in bacteria.^{22, 23, 24} Biomineralization fulfills a variety of crucial functions, including important skeletal and protective roles. The plant kingdom exhibits a varied assortment of mineralized structures formed by cells, including deposits of silica, calcium oxalate, and calcium carbonate.²⁵ Calcium oxalate crystals are by far the most prevalent and widely distributed mineral deposits in higher plants. Calcium is very abundant in the natural environment in which most plants grow.

A required element for plant growth and development, calcium plays many important roles, for example, as a structural component of cell walls, a signal in various physiological and developmental pathways.^{24,26} Nonetheless, cytosolic free calcium must be restricted to levels of 7M or less, because higher concentrations interfere with a variety of crucial cell processes, including calcium-dependent signaling, phosphate-based energy metabolism, and microskelatal dynamics.^{26, 27, 28} In addition, most plants, unlike animals, do not have well-developed excretory systems to dispose of excess calcium. Instead, higher plants appear to modulate differences between the natural abundance of environmental calcium and the very low levels required for cytosolic free calcium by controlling the distribution of calcium within the cell.^{29,30,31} The cell wall and the vacuole provide major sinks for calcium in plants. In water, calcium oxalate provides a relatively insoluble, metabolically inactive salt for calcium sequestration. Calcium oxalate thus provides a high-capacity repository for calcium, and plants may accumulate this salt in substantial amounts, up to 80% of their dry weight or 90% of total calcium.^{32,33} The extent of calcium partitioning into calcium oxalate varies among different taxonomic groups of plants.

1.2.1 Environmental and Economic Impact of Calcium Oxalate deposits

A good source of cellulose fibers (pulp) for making paper are trees, although alternative fibers like straw, hemp, and kenaf are used whenever possible. The trees are usually either ground up by mechanical force or soaked in chemicals to get more purified fibers. Traditionally, the bleaching of pulp has been effected through sequential reactions involving chlorine and sodium hydroxide. The early stages remove lignin; while the final stages brighten the pulp. Classes of bleaching chemicals include strong oxidizing agents

(Cl₂, O₃, NaOCl, ClO₂, O₂, and H₂O₂), and alkali (NaOH). Chlorine, chlorine dioxide and ozone work best when they are run in acidic conditions at pHs that range from 1.5 to 4. The presence of oxalic acid and divalent ions in plant makes it attractive to bleach in acidic condition which insures ion exchange between hydrogen ions and the divalent ions, thus, minimizes the chances of forming insoluble salt calcium oxalate according to the following reaction:



Due to recent regulations passed by the EPA to limit the use of chlorinated compounds, alternative routes are being implemented. The major problem with these alternative bleaching chemicals is that they favor formation of calcium oxalate, which forms scale deposits on the equipment of bleaching plants.

1.2.2 Calcium Oxalate as a Sparingly Soluble Salt

Calcium oxalate monohydrate (COM) is a sparingly soluble salt with a solubility product of 2.00×10^{-9} mole²/liter² at 25 °C.³⁴ COM precipitates from solution at low concentrations. The other kidney stone precipitates listed in Table 1.1 are also sparingly soluble salts (except for uric acid, uric acid monohydrate and l-cystine) and are also likely to precipitate from a solution containing relatively low concentrations of their respective constituent ions. Such a description is typical of sparingly soluble salts in general. Precipitates of these salts from low concentration solutions occur in various circumstances including industrial water systems and in the aforementioned biological phenomena. In particular, precipitates of the sparingly soluble salts calcium carbonate, CaCO₃, and calcium sulfate dihydrate, CaSO₄·2H₂O (gypsum), are often seen as unwanted scale in boilers, reactors, and cooling water systems. This scaling reduces heat transfer

coefficients and often leads to obstructions in piping. The removal of scale from process surfaces and the treatment of raw water to reduce its scaling tendency is done at considerable expense to industry. In order to develop cost-effective means of reducing scale as well as managing kidney stone treatment, it is desirable to search for compounds that inhibit formation of sparingly soluble calcium salt. Inhibitors of calcium salts are typically studied by considering the crystallization characteristics of the calcium salt.

1.3 Crystallization Kinetics

The control of crystallization is of fundamental importance in many biological and industrial processes; for instance in biomineralization, specific mineral polymorphs are selectively crystallized, while in pulp mills calcium oxalate forms deposits on the equipment of the bleach plant, for example in filtrate tanks and on washing filter wires. Controlled crystallization can be achieved only through an understanding of the crystallization at the molecular level.

Crystallization involves two distinct processes that are driven by supersaturation of the solute in the solvent: nucleation and crystal growth. There are two types of nucleation; primary and secondary nucleation, as illustrated in the Figure 1.1. In primary nucleation, no crystals are involved in the nucleation, whereas secondary nucleation is induced by crystal seeds. The main requirement of primary nucleation is supersaturation and it is the form of nucleation usually associated with the precipitation of calcium salt. In supersaturated solutions, solute units such as atoms, molecules or ions aggregate together to form a cluster or embryo. Such processes require energy, depending upon the surface/interfacial tension of the interface, to expel the solvent molecules. Therefore, the energy barriers associated with the cluster formation control nucleation kinetics as well as crystal habit. Once the cluster has reached a certain critical size, it becomes stable and serves as a nucleus for further growth or dissolves.³⁵

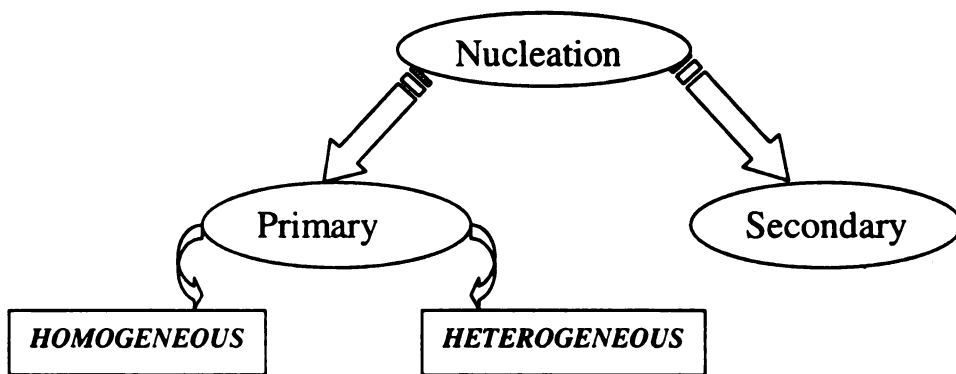


Figure 1.1

The different types of nucleation and the corresponding subcategories³³

1.3.1 Supersaturation

Understanding of the driving force for crystallization is essential for characterizing the kinetics as well as to regulate the parameters that control the crystal growth. The most important parameter that defines the crystallization process is supersaturation. Supersaturation is defined as the amount of solute in excess of the equilibrium solubility that is present in solution at a given temperature and is the driving force for the crystallization. The process of crystallization can be divided into two parts: nucleation and growth. Nucleation is energetically more demanding than crystal growth because there is an energy barrier associated with formation of stable nuclei. Consequently, there are supersaturation regions in which crystal growth proceeds while nucleation is suppressed.^{36,37,38}

The driving force for nucleation and growth is the difference in chemical potential of the solute in a supersaturated solution, μ_1 , and in a saturated solution, μ_{eq} . For an anhydrous solute crystallizing from a binary solution, the driving force may be written as $\Delta\mu = \mu_1 - \mu_{eq}$. Since, $\mu = \mu^o + RT \ln a$, then

$\Delta\mu = RT \ln (a_1/a_{eq}) = RT \ln (\gamma_1 C_1 / \gamma_{eq} C_{eq})$ and the supersaturation σ can be expressed in dimensionless terms by $\sigma = \Delta\mu / RT = \ln (a_1/a_{eq}) = \ln (\gamma_1 C_1 / \gamma_{eq} C_{eq})$.

If the ratio of the activity coefficient, γ_1 / γ_{eq} = constant in the given concentration regime, then the supersaturation becomes $\sigma = \ln (C_1/C_{eq}) = \ln (S_c + 1)$ where C is the concentration of the crystallizing substance in the supersaturated solution and $S_c = [(C_1 - C_{eq}) / C_{eq}]$. Normally, S_c is taken to be much less than unity as a

consequence $\sigma = \ln(S_r + 1) \equiv \left[\frac{(C_1 - C_{eq})}{C_{eq}} \right]$.³⁵

There are various methods to create supersaturation which include (a) solvent removal (evaporation or freezing), (b) addition of different salts with ions that participate in precipitation, and (c) dissolution of metastable solid phases. Supersaturation can also be created by methods that regulate the solute solubility, such as temperature change, pH change, and addition of a solvent that lowers the solubility of the solute.

1.3.2 Homogeneous Nucleation

The classical theory of nucleation based on the work by Gibbs,³⁹ Volmer,⁴⁰ and others, assumes that clusters are formed in solution by an addition mechanism that continues until a critical size is reached. The rate of nuclei formation (B_0) by this mechanism is given by an Arrhenius type expression

$$B_0 = A \exp\left(\frac{\Delta G_0}{\kappa T}\right) \quad (1.1)$$

where A is the pre-exponential factor and has a theoretical value of 10^{30} nuclei/cm³s. κ is the Boltzmann's constant, and T is temperature. The free energy change for an aggregate undergoing a phase transition, $\Delta G_0 = \Delta G_v + \Delta G_s$, where ΔG_v is the volume free energy change associated with the phase transition (a negative quantity), and ΔG_s is the surface free energy change associated with the formation of the aggregate (a positive quantity).

For homogeneous or heterogeneous nucleation

$$\Delta G_s = -\alpha r^3 \kappa T / v \ln(c/s) \quad (1.2)$$

where α is the volume-shape factor, r is the characteristic length, and v is the molecular volume of the crystallizing solute, and $\ln(c/s)$ is the supersaturation ratio. For homogeneous nucleation

$$\Delta G_s = \beta r^2 \gamma_{12} \quad (1.3)$$

where β is the area shape factor and γ is the interfacial energy per unit area between the crystallization medium, 1, and the nucleating cluster, 2. Due to the competition between volume and surface terms, ΔG_0 passes through a maximum at a certain value of r^* . The value of r^* can be obtained by minimizing the free energy function with respect to the characteristic length.

$$d(\Delta G)/dr = -3\alpha r^2 \kappa T / v \ln(c/s) + 2\beta r \gamma_{12} = 0 \quad (1.4)$$

The critical radius r^* of the cluster is given by:

$$r^* = \frac{2\beta v \gamma_{12}}{3\alpha \kappa T \ln(c/s)} \quad (1.5)$$

For spherical clusters, $\alpha=4\pi/3$ and $\beta=4\pi$. Therefore,

$$r^* = \frac{2v \gamma_{12}}{\kappa T \ln(c/s)} \quad (1.6)$$

Considering these geometric factors, the rate for homogeneous nucleation of spherical cluster is

$$B_0 = A \exp \left(\frac{-16\pi v^2 \gamma_{12}^3}{3(\kappa T)^3 \ln\left(\frac{c}{s}\right)^2} \right) \quad (1.7)$$

The equation above predicts that nucleation can be controlled experimentally by the following parameters: molecular or ionic transport, viscosity, supersaturation, solubility, solid-liquid interfacial tension, and temperature.

1.3.3 Heterogeneous Nucleation

Heterogeneous nucleation occurs at an interface, e.g foreign bodies or the walls of the retaining vessel. The critical supersaturation and the activation energy are considerably

lower than homogeneous nucleation. The rate of heterogeneous nucleation has the same form as that describing homogeneous nucleation above (1.6). Generally, any adsorption of foreign particles onto the nucleus decreases interfacial tension.⁴¹ Hence, an increase of nucleation rate is also observed. Impurities are also known to decrease the nucleation rate.⁴² A review of experimental work on heterogeneous nucleation is given by Tunbull and Vonnegut.⁴³

1.3.4 Crystal Growth Theory

Once the nucleation step has been achieved, nuclei grow into macroscopic crystals. This stage of the crystallization process is known as crystal growth. Crystal growth can be seen as a succession of events as proposed by Bennema:⁴⁴ a) transport of species from the bulk solution to a site at the crystal surface, b) adsorption of the growth unit to a site at the crystal surface, c) surface diffusion from the impingement site to a growth site, and, d) incorporation into the crystal lattice. Desolvation and/or solvent adsorption can take place in steps b-d. The rate-limiting step can be any of the above depending on the growth conditions such as the supersaturation, temperature, additives or solvent, and hydrodynamics of the system.

A few theories attempting to explain the growth of single crystals from solution have been proposed. Growth can be divided into two regimes, bulk solution mass transfer-limited growth and surface-integration limited growth.⁴⁵ Bulk solution mass transfer-limited growth theories presume that matter is deposited continuously on a crystal face at a rate proportional to the difference in concentration between the point of the deposition and the bulk of the solution, while surface integration theories are more complex.⁴⁶ The goals of crystal growth theories are to determine the source of steps and

the rate-controlling step for the crystal growth. If diffusion of solute from bulk solution to the crystal surface is rate limiting, growth is controlled by mass transfer. However, if incorporation into a crystal lattice is the slowest process, growth is controlled by surface-integration.

Depending on the roughness of the crystal surface, layer growth or continuous growth may result. Continuous growth model applies when the crystal-solution interface at the molecular level has many kink sites. If the interface is smooth, growth proceeds through a layer growth model: screw dislocation and two-dimensional nucleation. Details of the derivation of these models have received considerable attention in the literature.⁴⁷

1.3.4.1 Burton, Cabrera, and Frank Model (Screw Dislocation Model)

The spiral growth mechanism or screw dislocation model was first described by Burton, Cabrera, and Frank (BCF), who developed their theory for growth from the vapor, but theorized that a similar treatment would be applicable for growth from liquid solution.⁴⁸ Bennema modified this theory for crystals growing from aqueous solution.⁴⁹ The screw dislocation emerges on a crystal face provides a step or a sequence of steps over the surface for the addition of growth units (Figure. 1.2).

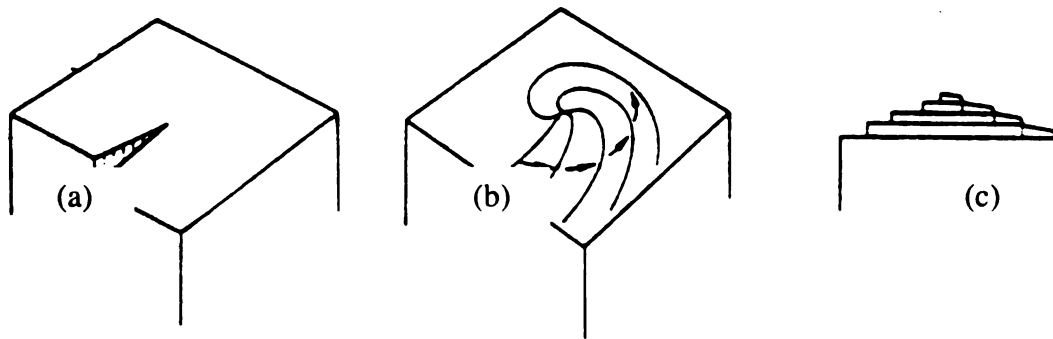


Figure 1.2

Development of a growth spiral starting from a screw dislocation (a) to spiral staircase (c)⁵⁰

The growth rate of a crystal face may be described by the following equation:

$$R = A \left(\sigma^2 / \sigma_a \right) \tanh (\sigma_a / \sigma) \quad (1.9)$$

where R is the growth rate of a crystal face, and A is a combination of physical constants of the system including adsorption, surface diffusion, and growth unit incorporation factors. At low supersaturations, where $\sigma \ll \sigma_a$, $\tanh (\sigma_a / \sigma) \rightarrow 1$, and the equation reduces to a form in which the growth is proportional to the supersaturation to the second power.

$$R = A \sigma^2 / \sigma_a \quad (1.10)$$

This is known as the parabolic rate law. At high relative supersaturations, where $\sigma \gg \sigma_a$, $\tanh (\sigma_a / \sigma) \rightarrow \sigma_a / \sigma$ and the BCF equation reduces to

$$R = A \sigma, \quad (1.11)$$

growth is linear with supersaturation.

The limitation of the BCF model is that, while it holds for growth from the vapor, it is difficult to quantify the model in growth from solutions due to the more complex nature of the systems. In solutions, sometimes the diffusion from the bulk solution to the interface may be the rate limiting step. For this case, the Chernov model is well known.⁵¹

The growth rate is given by

$$R = f \left\{ \sigma^2 / \left(1 + k \ln (\delta / y_0) \right) \right\} \quad (1.12)$$

where δ is the boundary layer thickness, and k depends on the diffusion coefficient, the kink density and the step height. At low σ , the equation behaves similarly to the BCF model. However, the growth rate decreases with an increase in δ .

1.3.4.2 Birth And Spread Model (Two-Dimensional Growth Of Surface Nuclei)

Another theory of crystal growth is the birth and spread model described by Hillig.⁵² As opposed to the BCF theory, this theory assumes that growth develops from surface nucleation that can occur at the edges, corners and on the faces of a crystal, as illustrated in Figure 1.3. Adsorbed growth units join an existing surface nucleus or form a new nucleus which then grows through the addition of other growth units. In further steps, 2D nucleus spreads across the surface. When a complete layer has formed, the crystal has grown by one monomolecular layer. The activation free energy for creating the 2D nucleus, if the nucleus is square, is $\Delta G = 4\lambda^2/\kappa_B T \ln \beta$, where λ is the edge free energy per molecule of the nucleus. For the mononuclear model where the whole crystal face is covered before the next nucleus forms, the growth rate of the face is $R = J_2 d S$, where J_2 is the 2D nucleation rate, d is the height of the layer, and S the area of the face.

In cases where several nuclei spread on the face at the same time, a polynuclear mechanism predicts a relationship between the face growth rate, and the supersaturation σ , as

$$R = A\sigma^{5/6} \exp(-B/\sigma) \quad (1.13)$$

At low relative supersaturations, the exponential term will dominate giving a region analogous to the parabolic region of the BCF curve. At high relative supersaturations, the exponential term approaches 1, leaving growth rate, R , proportional to $\sigma^{5/6}$; this is analogous to the linear region of the BCF curve.

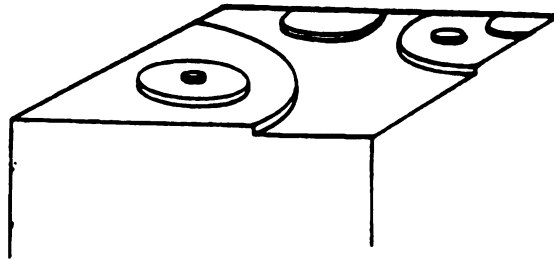


Figure 1.3

Depicts such a polycrystalline growth by the birth and spread (B+S) mechanism.^{37,52}

1.3.4.3 Diffusion-Controlled Growth

In the previous sections, we have dealt with the case where growth is controlled by surface integration, and the rate-limiting step was incorporation of a growth unit into the crystal lattice. Now we address a crystal growth rate for the case where the nucleation is quick in comparison to the time needed for the solute to diffuse to the surface, namely, diffusion-controlled growth. It is this model that is used in correlating data for industrial crystallization processes.

The basis of the diffusion-controlled growth is that solute diffuses from regions of higher concentration and is then incorporated into the crystal. On the assumption that there is a thin stagnant film of liquid adjacent to the growing crystal face, the rate of mass increase of the crystals ($\frac{dm_c}{dt}$) can be expressed as follows.⁴⁷

$$\frac{dm_c}{dt} = DA \left(\frac{dc}{dx} \right) \quad (1.14)$$

where A is the surface area of the crystal, and D is the diffusion coefficient. The concentration versus position through the boundary layer can be written as

$$\frac{dC}{dx} = \frac{C - C_i}{\delta} \quad (1.15)$$

where C and C_i are the bulk and interfacial concentrations, respectively. Substituting Eq. (1.15) into Eq. (1.14) yields

$$\frac{dm_c}{dt} = k_d (C - C_i) \quad (1.16)$$

where k_d is a coefficient of mass transfer by diffusion, D/δ .

The rate of solute integration into the crystal surface can be approximated by the relation

$$\frac{dm_c}{dt} = k_r A (C_i - C^*)^i \quad (1.17)$$

where i is between 1 and 2, k_r is the rate constant for the surface reaction integration process, and C_i is the interfacial concentration. Equation 1.17 is normally not applied because it involves the interfacial concentrations that are difficult to measure. Hence, it is usually more convenient to eliminate the C_i term by considering concentration driving force, $(C - C^*)$. A general equation for crystallization based on this overall driving force can be written as

$$\frac{dm_c}{dt} = k_g A \Delta C^g \quad (1.18)$$

where k_g is an overall growth coefficient and the g is the crystal growth order.

$$\frac{1}{k_g} = \frac{1}{k_d} + \frac{1}{k_r} \quad (1.19)$$

When $k_d \gg k_r$, the crystal growth rate will be diffusion controlled and $k_g = k_r$. On the other hand, when $k_r \ll k_d$, the crystal growth rate will be controlled by the rate of solute incorporation into the crystal.³⁷

If a chemical reaction is used to produce the insoluble species, the rate of reaction can be the rate-limiting step. A quantitative measure of the influence of resistance to growth is made through the concept of the effectiveness factor, η_c .⁵³ The effectiveness factor can be defined as

$$\eta_c = \frac{\text{growth rate observed at the interface}}{\text{growth rate when interface is exposed to bulk solution}}$$

which is a function of the Damköhler number, Da .

$$\eta_c = (1 - \eta_c Da)^r \quad (1.20)$$

where r is the order of the surface integration process.

$$Da = k_r (C - C^{eq})^{r-1} (1 - \omega) k_d^{-1} \quad (1.21)$$

where Da represents the ratio of the pseudo-first-order rate coefficient at the bulk conditions to the mass transfer, and ω is the mass fraction of solute in solution. When Da is large ($\eta_c \rightarrow Da^{-1}$) the growth is diffusion controlled, and when Da is small, the growth is surface integration controlled ($\eta_c \rightarrow 1$).

1.3.5 Crystal Shape

The external appearance of a crystal is the crystal habit, a property that can be controlled either thermodynamically or kinetically. Crystals grown at a very slow growth rate are usually thermodynamically controlled. In 1878, Gibbs proposed that the total free energy of a crystal in equilibrium with its surrounding at constant temperature and pressure would be a minimum for a given volume, i.e.:

$$d \sum_n A_n \gamma_n = \sum_n \gamma_n dA_n = 0 \quad (1.22)$$

where A_n is the area of the n th face. In 1901 Wulff stated that crystal faces would grow at rates proportional to their respective surface energies, where the equilibrium shape is determined by the ratio of the distance from the face, h_n , to the specific surface energies,

$\frac{h_n}{\gamma_n}$.⁵⁴ A schematic representation of this equilibrium shape is shown in Figure 1.4.

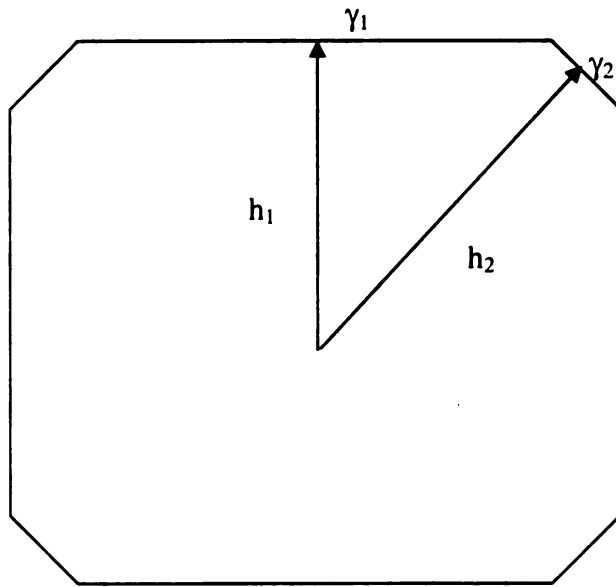


Figure 1.4

Equilibrium crystal shape as described by Wulff's theorem. In this case $\gamma_1 < \gamma_2$.⁵⁵

Essentially, an equilibrium shape crystal grows to maintain geometric similarity. Hartman and Perdok developed morphological theory that related bond energies to internal structures of crystal morphology.⁵⁶ They theorized that crystal growth is controlled by the formation of strong bonds between crystallizing particles called periodic bond chains (PBC). Growth layers of the periodic bond chains form three different crystal faces as shown in figure 1.5. The F-face (flat) is the elementary faces that grow slice after slice and is parallel to at least two PBC vectors. The S-face (stepped) parallel to at least one PBC vector. The K-faces (kinked) not parallel to any PBC vector, which needs no nucleation for growth. The rougher S- and K-faces grow very quickly, and it is rarely observed. On the other hand, the growth velocity of the F-face is very slow. Thus, the crystal habit is usually dominated by the F-face.

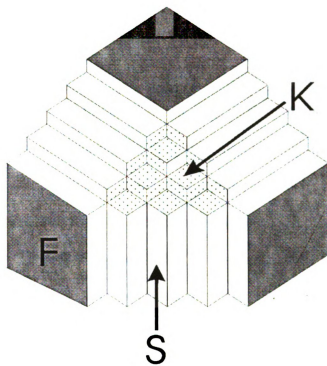


Figure 1.5

Hypothetical three-dimensional crystal presenting the three main types of possible faces: flat (F), step (S) and kink (K) faces.⁵⁷

1.3.6 Crystal Habit Modification

The observed habit of crystals grown from solution is often quite different from the prediction by the models mentioned previously. For crystals grown in solution, their shape will depend on kinetic factors which are affected by crystal defects, surface roughening, solvent type, supersaturation, temperature, impurities in the solvent and other solution conditions. These environmental conditions affect the growth of a given face. Some faces grow very fast and have little or no effect on the growth form; the ones that have most influence are the slow-growing faces. The most important technique used today for influencing habit modification is the addition of impurities, which preferentially adsorb on a specific crystal face. The first documented example of crystal habit modification was described in 1783 by Romé de L'Isle.⁵⁸ Urine was added to a saturated solution of NaCl, which resulted in changing the crystal habit from cubic to octahedral. The effect of organic impurities on the growth of inorganic crystals from aqueous solution was studied by Buckley as well.⁵⁹ In addition, the influence of impurities and solvents on crystallization has been discussed extensively by D.L. Klug.⁴⁵

Impurities which modify crystal habit fall into the following categories: ions, either anions or cations, ionic surfactants, either anionic or cationic, nonionic surfactants like polymers, and chemical binding complexes. These impurities all have propensity to adsorb on a specific crystal surface.⁶⁰ The specific surface energy, γ , that results from the adsorption of Γ atoms (or ions) per unit area is given by Gibbs⁶¹ as

$$-d\gamma = \Gamma \kappa T \ln(a_2) \quad (1.25)$$

where a_2 is the activity of the impurity. If crystal growth was mainly dependent on thermodynamic factors, then impurity adsorption should increase the growth rate of a

face because adsorption decreases the edge free energy. However, impurities affect kinetic factors much more than thermodynamic factors by inhibiting crystal growth. When only a few kinks are blocked on the surface, growth rate can be slowed down by several orders of magnitude.⁶² Therefore, additives or impurities may be very active at low concentrations. In general, their efficiency depends on their concentration. However, an increase in supersaturation reduces their efficiency.⁶³ According to Mullin et al.,⁶⁴ impurity ions in the vicinity of the surface will reduce the effective surface supersaturation, retard diffusion, and hinder the aggregation of growth units.

Ionic surfactant impurities are routinely used in industry to control crystal morphology during crystallization. As shown in Figure 1.6, anionic surfactants will adsorb on the negatively charged surfaces of adipic acid and limit their growth, giving plate-like crystals, while cationic surfactants will adsorb on the positively charged surfaces of adipic acid crystals and limit their growth, giving needle-like crystals.

Tailor-made impurities are an important class of impurities (additives) which are designed to interact in very specific ways with selected faces of crystalline material. Basic strategies for designing crystallization additives are (i) mimicking the solute molecule (e.g., chemical groups or moieties) such that they can readily adsorb at growth sites on the crystal,⁶⁵ (ii) introducing steric hindrance to disrupt subsequent growth processes on the affected faces,⁶⁶ and (iii) establishing chemical differences at the interface of growing crystal.⁶⁷

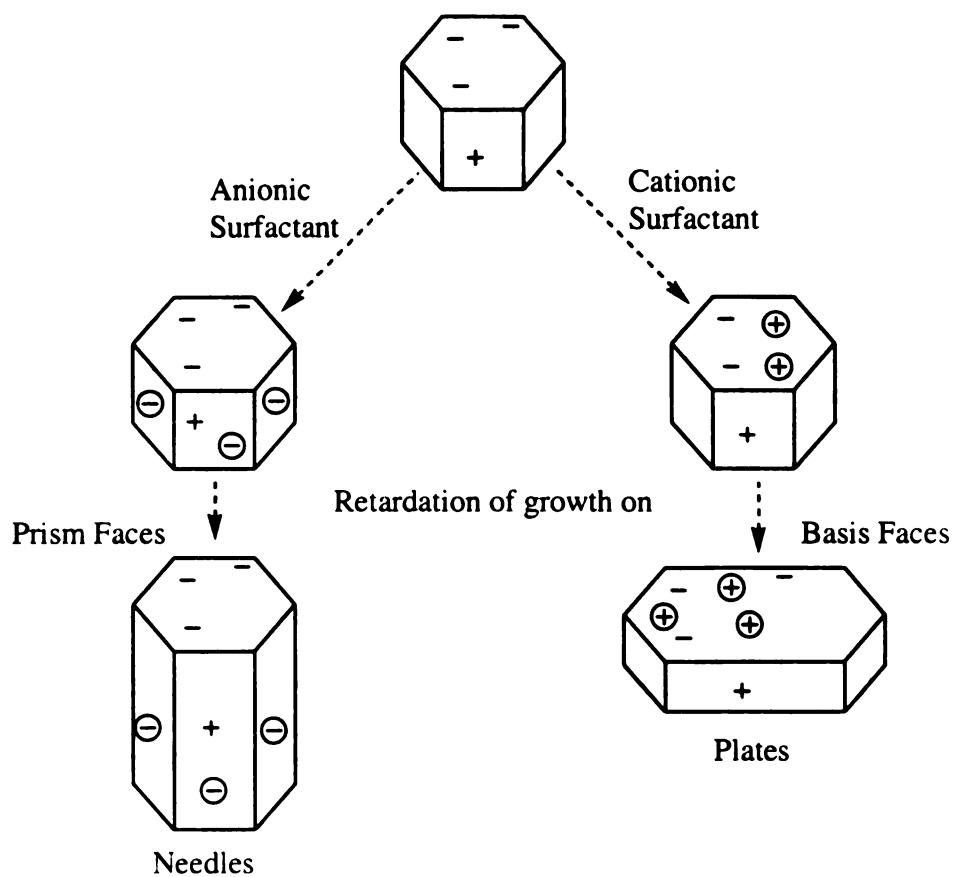


Figure 1.6

Influence of impurity adsorption on the crystal habit, for the case of adipic acid.⁵⁵

1.3.7 Phase Transformation

Phase transformations occur through four schemes: solid state, melt mediation, interface mediation, and solution mediation. Phase changes between solid structures involve rearrangement of molecules or atoms in the metastable solid such that the complete transformation occurs in the solid state.⁶⁸ From a kinetic point of view, solid state phase transformation is slower in comparison to other schemes due to the large activation energy of nucleation and growth required. However, phase transformation through the melt, interface, and solution can reduce the total activation energy for a complete polymorphic conversion to take place. The driving force of these transformations is the difference in chemical potential between the polymorphs. Such transformations are an inevitable consequence of the thermodynamic driving force toward minimizing the free energy of the system.

Kinetic factors involved in phase transformations include (i) nucleation and growth of the more stable form, (ii) dissolution, evaporation or melting of the less stable form, and (iii) mass transfer in the medium.^{69, 70} This concept is illustrated in figure 1.7 for solution-mediated phase transformation for two crystalline phases. The relative supersaturation, σ , defines a driving force for nucleation of each phase and crystal growth on existing surfaces. The rates of nucleation and crystal growth of each phase depend on the magnitudes of specific rate constants, interfacial energies, free energies of formation, solute diffusivity, and mixing intensity. The transformation time is limited by the dissolution of phase 1 crystals at their maximum dissolution rate, τ_D , and the rate of growth of phase 2 crystal at their maximum growth rate, τ_G . Thus, the transformation can be represented as the sum of the growth and dissolution times, $\tau = \tau_G + \tau_D$. If

$\tau_D \gg \tau_G$, the system can be said to be dissolution controlled and similarly if $\tau_D \ll \tau_G$ the system is growth controlled.

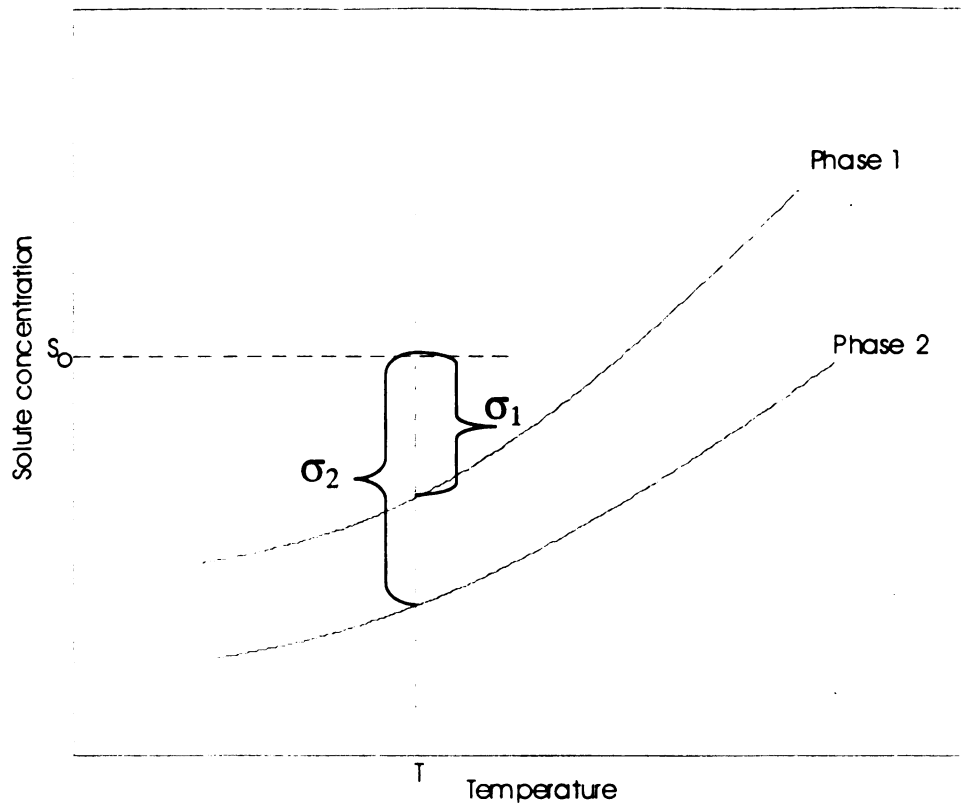


Figure 1.7

Typical solubility profiles and pertinent supersaturation values.⁷¹

1.4 REFERENCES

- ¹Watts, R. W. *Journal Of The Royal College Of Physicians Of London* **1973**, 7, 161-174.
- ²Boyce, W. H. *Amer. J. Med.* **1968**, 45, 673-683.
- ³Rose, G. A. *Urinary stones : clinical and laboratory aspects*; Lancaster, **1982**.
- ⁴Heijnen, W. M. M. *J. Cryst. Growth* **1982**, 57, 216-232.
- ⁵Heijnen, W.; Jellinghaus, W.; Klee, W. E. *Urol. Res.* **1985**, 13, 281-283.
- ⁶Fleisch, H. *Kidney International* **1978**, 13, 361-371.
- ⁷Robertson, W. G.; Peacock, M.; Marshall, R. W.; Marshall, D. H.; Nordin, B. E. *New England Journal Of Medicine* **1976**, 294, 249-252.
- ⁸Coe, F. L.; Parks, J. H. *Nephrolithiasis : pathogenesis and treatment*; 2nd ed.; Year Book Medical Publishers: Chicago, **1988**.
- ⁹Coe, F. L.; Favus, M. J. *Disorders of bone and mineral metabolism*; Raven Press: New York, **1992**.
- ¹⁰Finlayson, B. *Kidney International* **1978**, 13, 344-360.
- ¹¹Walton, A. G. *The formation and properties of precipitates*; Interscience Publishers: New York, **1967**.
- ¹²Finlayson, B. *Kidney International* **1978**, 13, 344-360.
- ¹³Robertson, W. G.; Peacock, M.; Marshall, R. W.; Marshall, D. H.; Nordin, B. E. *New England Journal Of Medicine* **1976**, 294, 249-252.
- ¹⁴Robertson, W. G.; Peacock, M.; Nordin, B. E. *Clinical Science* **1968**, 34, 579-594.
- ¹⁵Robertson, W. G.; Peacock, M.; Nordin, B. E. *Clinical Science* **1971**, 40, 365-374.
- ¹⁶Boyce, W. H. *Amer. J. Med.* **1968**, 45, 673-683.
- ¹⁷Hallson, P. C.; Rose, G. A. *Lancet* **1979**, 1, 1000-1002.
- ¹⁸Fleisch, H. *Kidney International* **1978**, 13, 361-371.

- ¹⁹Drach, G. W.; Sarig, S.; Randolph, A. D.; Thorson, S. *Urological Research* **1982**, *10*, 165-168.
- ²⁰Robertson, W. G.; Scurr, D. S.; Bridge, C. M. *J. Cryst. Growth* **1981**, *53*, 182-194.
- ²¹Ryall, R., Harnett, R., and Marshall, V., *J. Urology*, **1986**, 135, 174.
- ²²Anderson, H.C., *Clin.Orthop. Relat. Res.*, **1995**, 314, 266–280
- ²³Li, C.W., and Volcani, B.E., *Trans. R. Soc. Lond. B*, **1984.**, 304, 519-528
- ²⁴Bazylinski, D.A., Garratt-Reed, A.J., and Frankel, R.B., *Microsc. Res. Tech.*, **1994**, *27*, 289-401.
- ²⁵Arnott, H.J., and Pautard, F.G.E., *Calcification in plants. In Biological Calcification: Cellular and Molecular Aspects*. H. Schraer, ed (New York: Appleton-Century-Crofts), **1970**, 375–446
- ²⁶Bush, D.S., *Annu. Rev. Plant Physiol. Plant Mol. Biol.*, **1995**, *46*, 95–122.
- ²⁷Kretsinger, R.H., *Evolution of the informational role of calcium in eukaryotes. In Calcium-Binding Proteins and Calcium Function*, R.H. Wasserman, R.A. Corradino, E. Carafoli, R.H. Kresinger, D.H. MacLennan, and F.L. Siegel, eds (New York: North Holland), **1977**, 63–72.
- ²⁸Hepler, P.K. , *Cell Calcium*, **1994**, *16*, 322.
- ²⁹Clarkson, D.T., *Plant Cell Environ.*, **1984**, *7*, 449.
- ³⁰Kinzel, H., *Flora*, **1989**, 182, 99.
- ³¹Leigh, R.A., and Tomos, A.D., *Trans. R. Soc. Lond. B.*, **1993**, 341, 75.
- ³²Zindler-Frank, E., *Pflanzenphysiol*, **1975**, *77*, 80.
- ³³Fink, S., *New Phytol.*, **1991**, 119, 33.
- ³⁴Nancollas, G. and Gardner, G., *J. Crystal Growth*, **1974**, *21*, 267.
- ³⁵C. Phillip and Wankart, *Rate Controlled Separations*; Elsevier Applied Science Publishing Co., Inc., New York, **1990** Chapter 3.
- ³⁶Nyvtl, J.; Sohnel, O.; Matuchova, M.; Broul, M. *The Kinetics of Industrial Crystallization*; Elsevier: New York, **1985**.

- ³⁷Mullin, J. W. *Crystallization*; Butterworth-Heinemann Ltd.: Oxford, **1993**.
- ³⁸Sohnel, O.; Garside, J. *Precipitation: Basic Principles and Industrial Applications*; Butterworth-Heinemann Ltd: Oxford, **1992**.
- ³⁹Gibbs, J.W. , *Collected Works, Vol. I, Thermodynamics*, Yale University Press: New Haven, **1948**.
- ⁴⁰Volmer, M. , *Kinetic Der Phasenbildung*, Steinkopff, Leipzig, **1939**.
- ⁴¹Mutaftschiev, B., *Critical Rev. Solid State Sci.*, **1976**, 6, 157.
- ⁴²Lacmann, R., and Stranski, I. N., *Growth and Perfection of Crystals*, Roberts, B.W. Doremus, R. H., and Turnbull, D., Wiley, New York, **1958**, 427.
- ⁴³Turnbull, D., and Vonnegut, B., *Ind. Eng. Chem.*, **1952**, 44, 1292.
- ⁴⁴Bennema, P., *J. Crystal Growth*, **1967**, 1, 278.
- ⁴⁵Myerson, A. S., *Handbook of Industrial Crystallization*, Edt. Myerson, A. S. Butterworth-Heinemann. Boston, **1993**.
- ⁴⁶Noyes, A.A. and Whitney, W.R., *J. American Chemical Society*, **1897**, 19, 930.
- ⁴⁷Myerson, A. S., *Handbook of Industrial Crystallization*, Edt. Myerson, A. S. Butterworth-Heinemann. Boston, **1993**. Mullin, J. W., *Crystallization*, Butterworth-Heinemann Ltd., Oxford, **1993**, Chernov, A. A., *Contemp. Phys.* **1989**, 30, 252. Chernov, A. A., *Modern Crystallography III: Crystal Growth*, Springer-Verlag: Berlin, **1980**, Bennema, P., *J. Crystal Growth*, **1984**, 69, 182.
- ⁴⁸Burton, W. K.; Cabrera, N.; Frank, F. C., *Philos. Trans.*, **1951**, A243, 299.
- ⁴⁹Bennema, P., *J. Crystal Growth*, **1984**, 69, 182, Bennema, P., *J. Crystal Growth*, **1967**, 1, 225.
- ⁵⁰Mullin, J. W., *Crystallization*, Butterworth-Heinemann, Oxford, **1993**. Chaps. 6.
- ⁵¹Chernov, A.A., *Sov. Phys. Usp.*, **1961**, 4, 129.
- ⁵²Hillig, W., *Acta Met.*, **1966**, 14, 1968.
- ⁵³Garside, J., and Tavare, N.S., *Chem. Eng. Sci.*, **1981**, 40, 1485.
- ⁵⁴Wulff, G; *Z Kristallogr.*, **1901**, 34, 449

- ⁵⁵Nielsen, A. E. *Kinetics of precipitation*; Pergamon Press; Oxford, New York., **1964**.
- ⁵⁶Hartman, P.; Perdok, W. G. *Acta Cryst.* **1955**, 8, 525-9.
- ⁵⁷Elwell, D.; Scheel, H. J. *Crystal growth from high-temperature solutions*; Academic Press: London ; New York, **1975**.
- ⁵⁸Romé de L'Isle, *Cristallographie*, 2nd edition, Paris, **1783**, 379.
- ⁵⁹Buckley, H.E., *Crystal Growth*, Wiley, New York, **1951**.
- ⁶⁰Adamson, A.W., *Physical Chemistry of Surfaces*, 4th Edition, Wiley-Interscience. New York, **1982**.
- ⁶¹Gibbs, J.W., *Collected Works*, Longmans, Green, New York, **1928**.
- ⁶²Burrill, K.A., *J. Crystal Growth*, **1972**, 12, 239.
- ⁶³Boistelle, R. and Astier, J.P., *J. Crystal Growth*, **1988**, 90, 14.
- ⁶⁴Mullin, J.W. and Leci, C.L., *Eng. Prog. Symp.: Nucleation Phenomena*, 3rd, Joint Meeting AIChE and IMIQ, Denver, Colorado. August **1970**, Paper 39a.
- ⁶⁵Addadi, L., Berkovitch-Yellin, Z., Weissbuch, I., *Angewandte Chemie Int.*, **1985**, 24, 466.
- ⁶⁶Berkovitch-Yellin, Z. *J. Am. Chem. Soc.*, **1985**, 107, 8239.
- ⁶⁷Weisinger-Lewin, Y., Frolow, F., McMullan, R. K, *J. Am. Chem. Soc.* **1985**, 111, 1035.
- ⁶⁸Bamford, C.H. and Tipper, C.F.H., *Comprehensive chemical kinetics*, Amsterdam. Elsevier, **1980**, vol. 22.
- ⁶⁹Cardew, P. T. and Davey, R.J. *Proc. R. Soc. Lond.*, **1985**, A398, 415.
- ⁷⁰Sato, K., *J. Phys. D: Appl. Phys.* , **1993**, 26, B77.
- ⁷¹Thompson, R.W. and Dixon, A.G. *Proc. R. Soc. Lond.*, **1987**, A413, 369-381

Chapter 2

SYNTHESIS OF SIMPLE ORGANIC CHELATES DERIVED FROM AMINO ACID AND EPOXYSUCCINIC ACID FOR INHIBITION OF CALCIUM OXALATE CRYSTAL GROWTH

The crystallization of calcium oxalate in the presence of different additives was studied at ambient temperature. Citric acid, aliphatic amino acids, basic amino acids, and acidic amino acids derivatized with cis-epoxysuccinic acid were studied. Particle formation during the crystallization of calcium oxalate was monitored by nephelometry. The Savitsky-Golay algorithm was used to smooth the desupersaturation data and the data were subsequently used to estimate nucleation and growth kinetics. Induction times were determined and used as an indicator for the abilities of the additives as nucleation inhibitors. The percentage inhibition produced by the additives was calculated from the slopes of the crystallization curve as $[1 - (S_i/S_C)] \times 100$. The most effective inhibitor of both nucleation and crystal growth was the lysine derivative, leading to an inhibition of 98%, followed by citric acid. The aliphatic amino acid and the basic amino acid derivatives inhibited less than 50% crystal growth. The chelation strengths of the amino acid derivatives were determined by calcium ion selective electrode. The experimentally determined chelation constants were statistically equal to that of citrate, which leads us to believe that the inhibition properties of the lysine derivative as well as citrate are independent of their chelation properties.

2.1 INTRODUCTION

An answer to current environmental concerns is a detergent that biodegrades to CO_2 and H_2O and in addition to being non-toxic, is inexpensive to produce. Compounds with polycarboxylic acid groups make good ligands for calcium. Amino acids make good starting material for preparation of polycarboxylic acids because it contains a primary amine group which be attached to other molecules. These compounds could then be applied as detergent additives, as well as inhibitors of scale deposits, and kidney stone formation.

In the pulp and paper industries, calcium oxalate (CaC_2O_4) is notorious for forming scale deposits on the equipments.¹ Scale deposit in water-containing systems such as pipelines and air conditioning systems is another major area of concern. Water is recycled in many cooling water systems; however, this practice increases scaling tendencies. Therefore, an effective inhibitor of scale forming salts which also addresses the environmental concerns is a sensible approach to controlling scale deposits and steel corrosion.

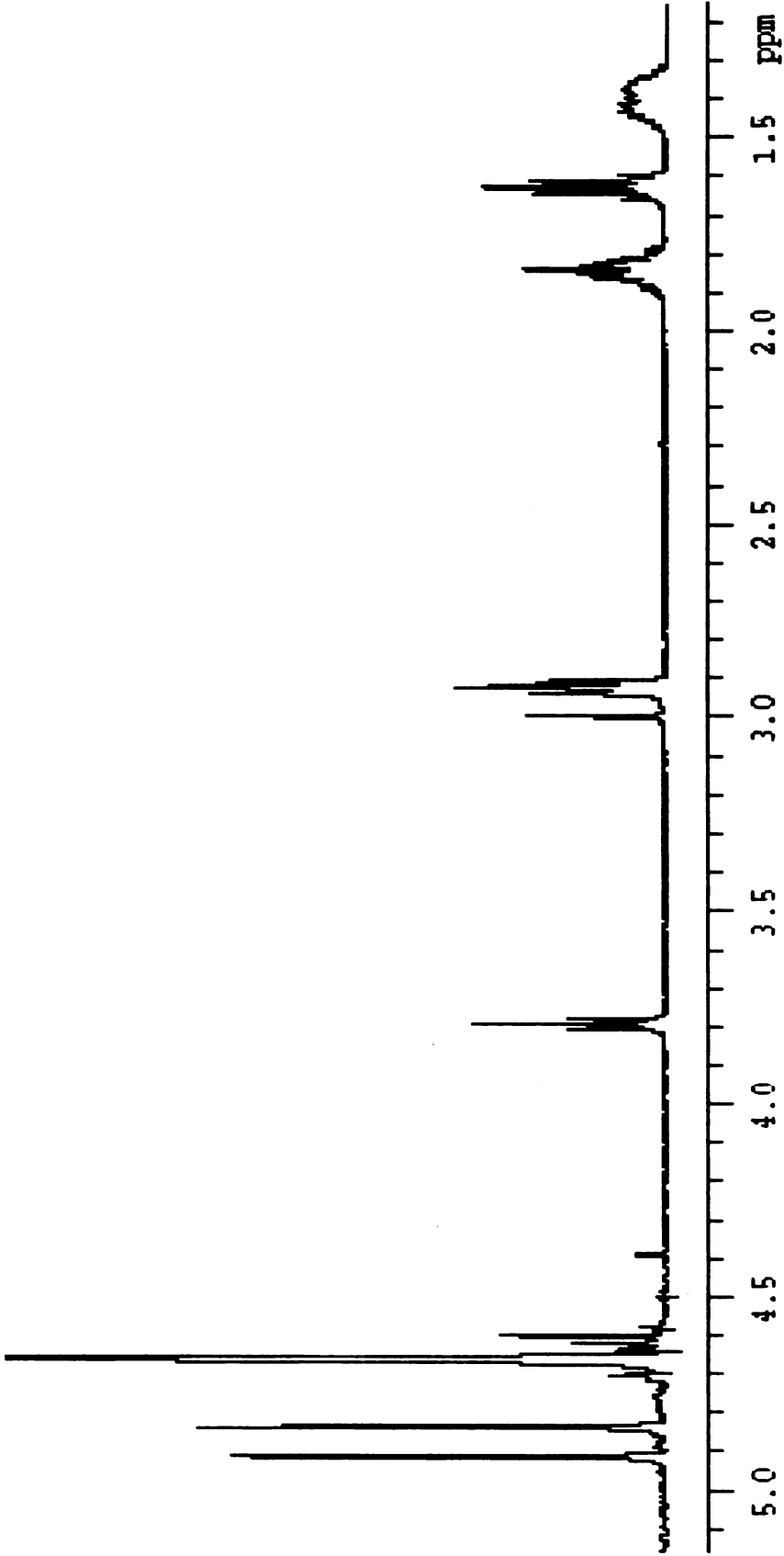
In animals, CaC_2O_4 occurs as a crystal in the urinary tract and constitutes the largest composition in kidney and bladder stones.² Calcium oxalate crystallizes in three hydrates: the monohydrate, the dihydrate, and the trihydrate, depending on solution conditions. The monohydrate phase is the main component of the most abundant type of renal calculi that is also the most difficult to treat and the most poorly understood.³ One form of clinical management of kidney stones is oral administration of citric acid supplements, which are inhibitors of calcium salt crystallization. Unfortunately, the

amount of citrate that must be consumed for effect is relatively large (in excess of grams per day, 2 to 8 grams/day).⁴

The factors that determine calcium salt formation include supersaturation and the resulting crystallization kinetics.⁵ When the solubility product of a calcium salt is exceeded, nucleation and crystal growth takes place, leading to stone formation or scale deposits.⁶ An effective inhibitor delays or prevents crystal growth. Amino acids were modified with cis-epoxysuccinic acid to create polycarboxylates with the intention of finding inhibitory compounds that were effective at concentrations less than citric acid. Subsequently, the crystallization of calcium oxalates in the presence of the derivatized amino acids was studied at ambient temperature. In addition, the chelation properties of the derivatives were also determined.

recorded using a 300-MHz Varian INOVA spectrometer. Mass Spectrometry analysis was attempted but the results were inconclusive. Consequently, only the NMR was used as the definitive method of choice.

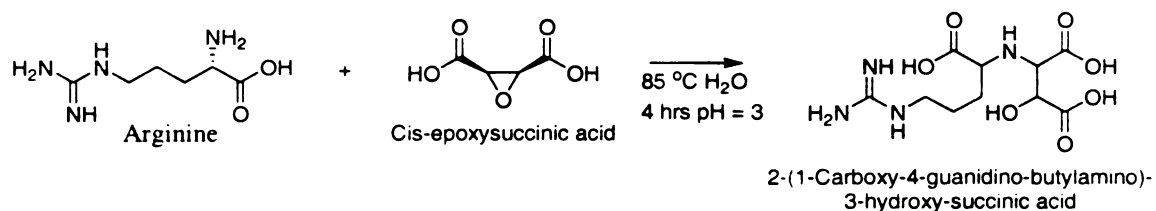
Lysine derivative $^1\text{H-NMR}$ (300 MHz, D_2O @ 40 °C): (ppm) = 1.400 (m, 2H); 1.628 (m, 2H); 1.840 (m, 2H); 2.923 (m, 2H); 3.793 (m, 1H); 4.660 (dd, 1H); and 4.662 (dd, 1H).



Spectrum 2.1

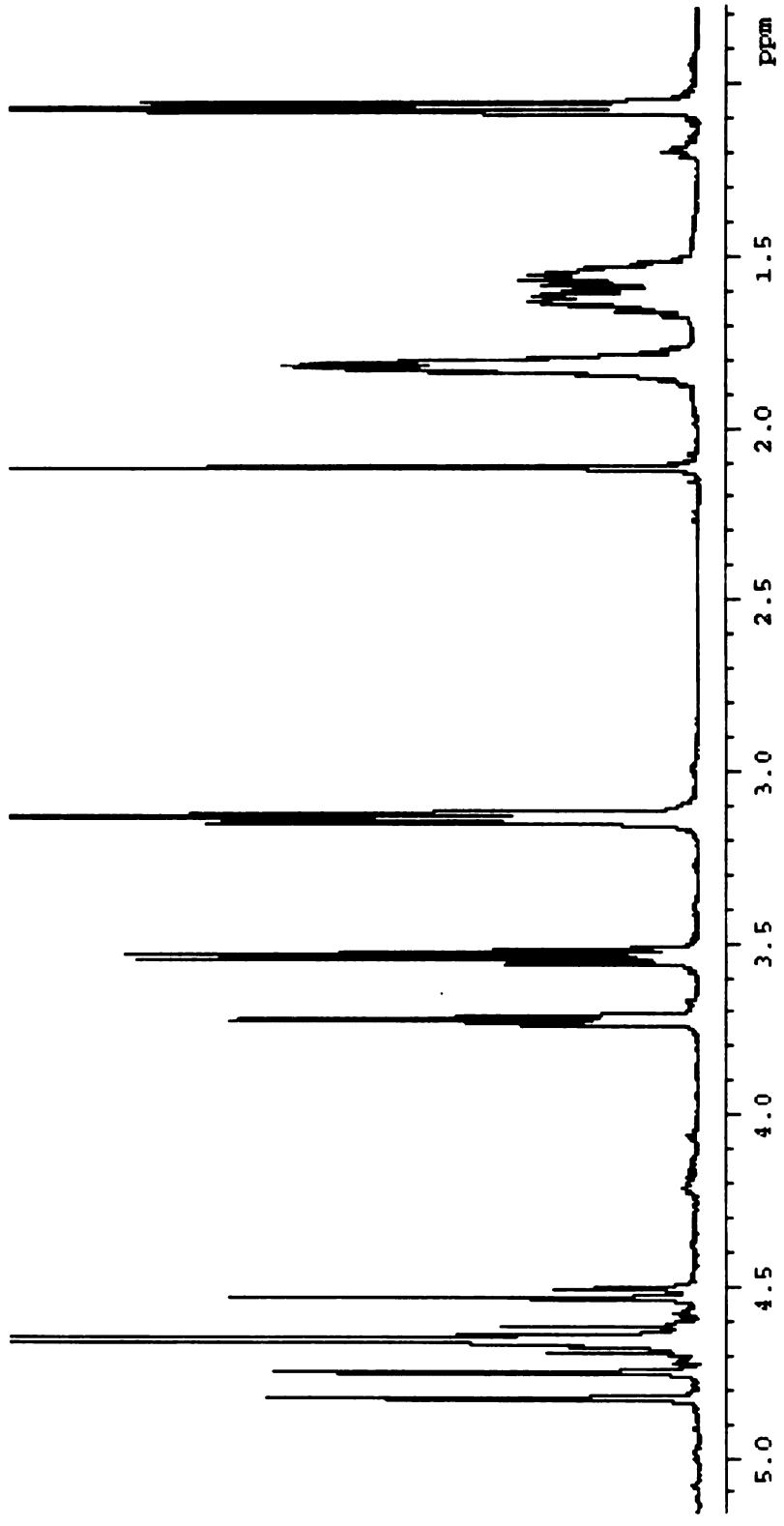
¹H-NMR spectrum of lysine derivative (2,6-Bis-(1,2-dicarboxy-2-hydroxy-ethylamino)-hexanoic acid)

Scheme 2.2 Synthesis of arginine derivative (2-(1-Carboxy-4-guanidino-butylamino)-3-hydroxy-succinic acid)



L-arginine hydrochloride, 2.39g (0.01136 moles), was added to 5 mL of deionized water containing 1.5g (0.01136 moles) of cis-epoxysuccinic acid. The reaction mixture was refluxed at 80 °C for 4 hours under nitrogen atmosphere and allowed to cool to room temperature. Ethanol was added into the solution until two immiscible liquid formed. The top liquid ethanol/water azeotrope was decanted off and the remaining filtrate is repeatedly washed with ethanol followed by acetone to remove unreacted epoxysuccinic acid. The product was characterized by ¹H NMR in D₂O. The NMR was recorded using a 300-MHz Varian INOVA spectrometer. Mass Spectrometry analysis was attempted but the results were inconclusive. Consequently, only the NMR was used as the definitive method of choice.

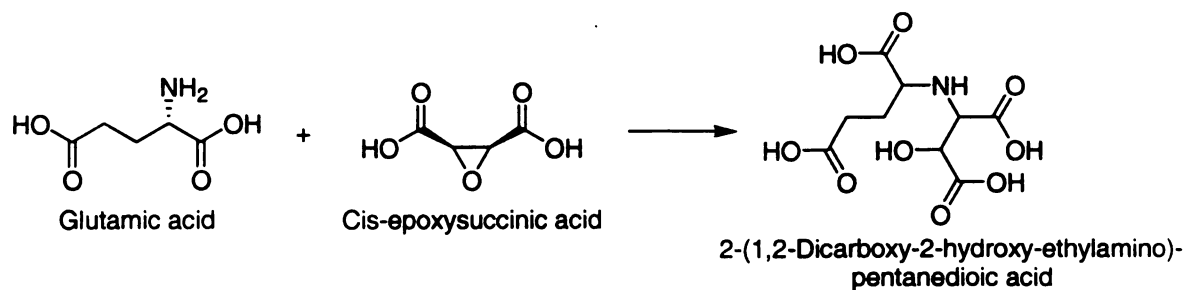
Arginine derivative ¹H-NMR (300 MHz, D₂O @ 40 °C): (ppm) = 1.560 (m, 2H); 1.820 (m, 2H); 3.138 (m, 2H); 3.724 (m, 1H); 4.752 (dd, 1H); and 4.791 (dd, 1H).



Spectrum 2.2

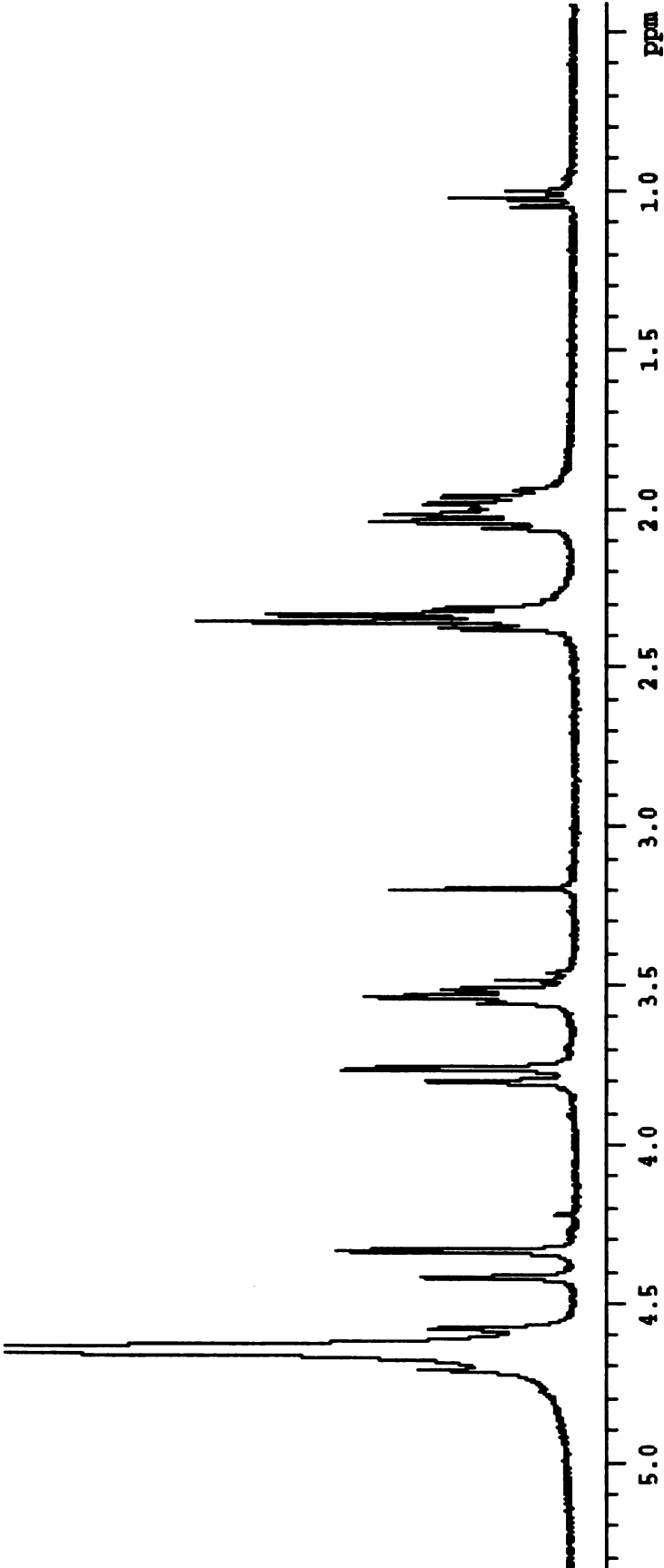
¹H-NMR spectrum of arginine derivative (2-(1-Carboxy-4-guamido-butylamino)-3-hydroxy-succinic acid)

Scheme 2.3 Synthesis of glutamic derivative (2-(1,2-Dicarboxy-ethylamino)-pentanedioic acid)



L-glutamic acid (1.67g, 0.01136 moles) in water was titrated with 1M NaOH to pH 9.7 which corresponds to the pK_a of the α -amino group. Epoxysuccinic acid (1.50g, 0.01136 moles) was added, upon which the pH dropped to less than 4. Base was added to return the pH to 9.7. The mixture was heated in an oil bath at 80 °C for 4 hours in a flask attached to a reflux condenser. After allowing the reaction mixture to cool to room temperature, ethanol was added into the solution until two immiscible liquids formed. The supernatant was decanted off and the filtrate was repeatedly washed with ethanol. The amorphous sample was crystallized by titrating it to \approx pH 4 with concentrated HCl. A Buchner filter funnel with medium frit was used to isolate the crystallized product. To remove any impurities such as tartaric acid or epoxysuccinic acid, the amino derivative was washed in methanol. The unreacted amino acid was removed by dissolving the sample in water which resulted in crystallization of the amino acid. After drying, the product was characterized by ^1H NMR. Mass Spectrometry analysis was attempted but the results were inconclusive. Consequently, only the NMR was used as the definitive method of choice.

Glutamic derivative $^1\text{H-NMR}$ (300 MHz, D_2O @ 25 °C): 2.007 (m, 2H-C(4')); 2.343 (m, 2H-C(3')); 3.530 (m, 1H-C(2')); 3.756 and 3.802 (dd, 1H-C(2)); 4.333 and 4.416 (dd, H-C(3)).

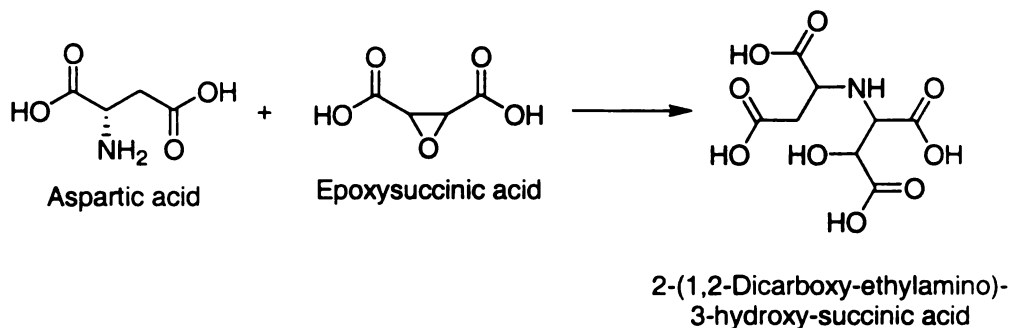


Spectrum 2.3

¹H-NMR spectrum of glutamic derivative (2-(1,2-Dicarboxy-ethylamino)-pentanedioic acid)

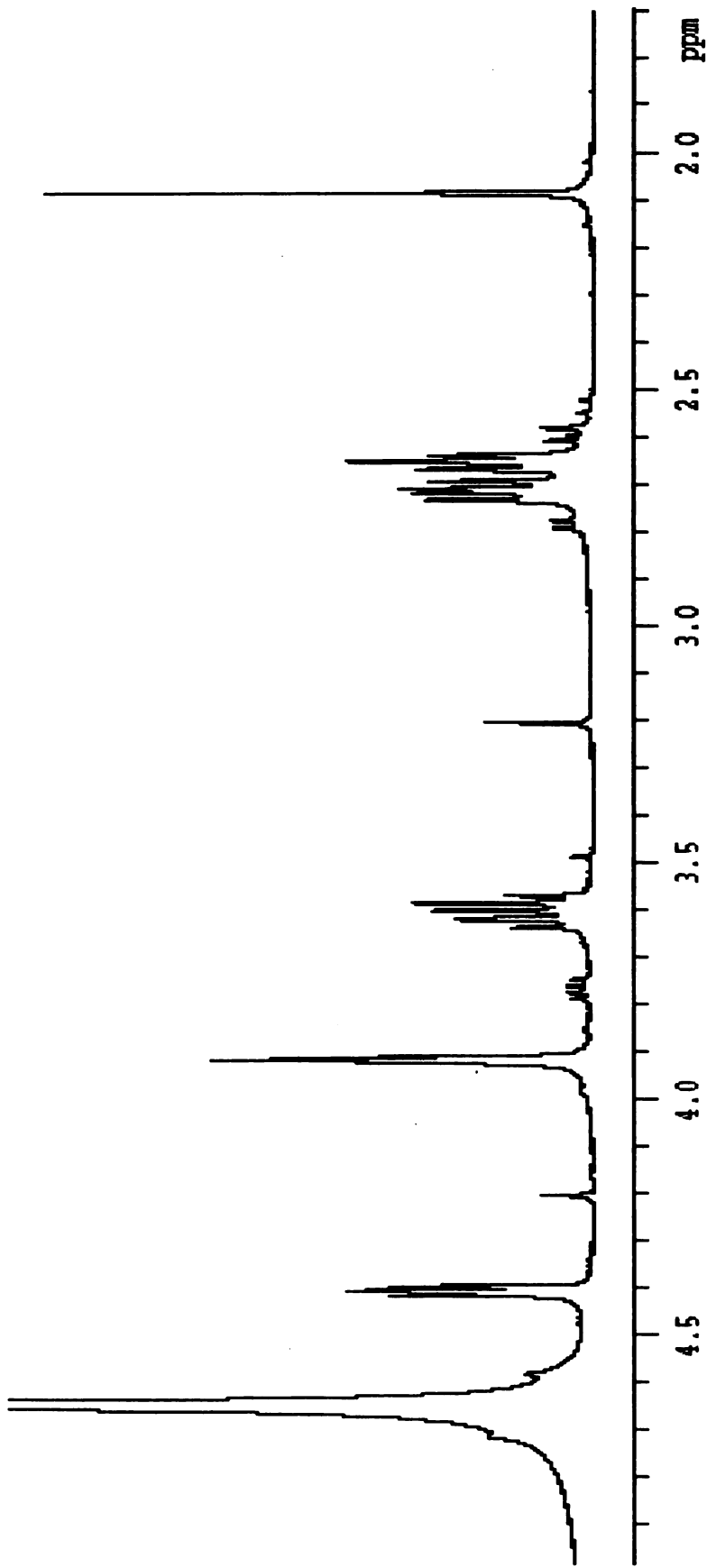


Scheme 2.4 Synthesis of aspartic derivative (2-(1,2-Dicarboxy-ethylamino)-3-hydroxy-succinic acid)



L-aspartic acid (1.51g, 0.01136 moles) in water was titrated with 1M NaOH to pH 9.8 which corresponds the pK_a of the α -amino group. Epoxysuccinic acid (1.50g, 0.01136 moles) was added, upon which the pH dropped to less than 4. Base was added to raise the pH to 9.8. The mixture was heated in an oil bath at 80 °C for 4 hours in a flask attached to a reflux condenser. After allowing the reaction mixture to cool to room temperature, ethanol was added into the solution until two immiscible liquids formed. The supernatant was decanted off and the filtrate was repeatedly washed with ethanol. The amorphous sample was crystallized by titrating it to \approx pH 4 with concentrated HCl. A Buchner filter funnel with medium frit was used to isolate the crystallized product. To remove any impurities such as tartaric acid or epoxysuccinic acid, the amino derivative was washed in methanol. The unreacted amino acid was removed by dissolving the sample in water which resulted in crystallization of the amino acid. After drying, the product was characterized by ^1H NMR in D_2O . Mass Spectrometry analysis was attempted but the results were inconclusive. Consequently, only the NMR was used as the definitive method of choice.

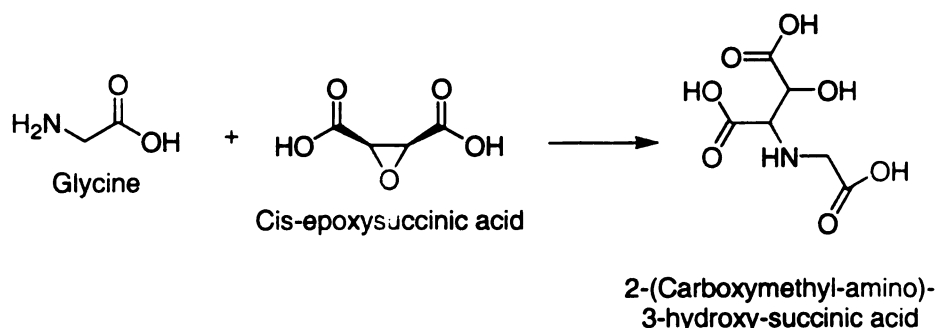
Aspartic derivative $^1\text{H-NMR}$ (300 MHz, D_2O @ 25 °C): 2.656 and 2.715 (mm, 2H-C(3')); 3.605 (m, 1H-C(2')); 3.920 (d, 1H-C(2)); and 4.410 (d, 1H-C(3)).



Spectrum 2.4

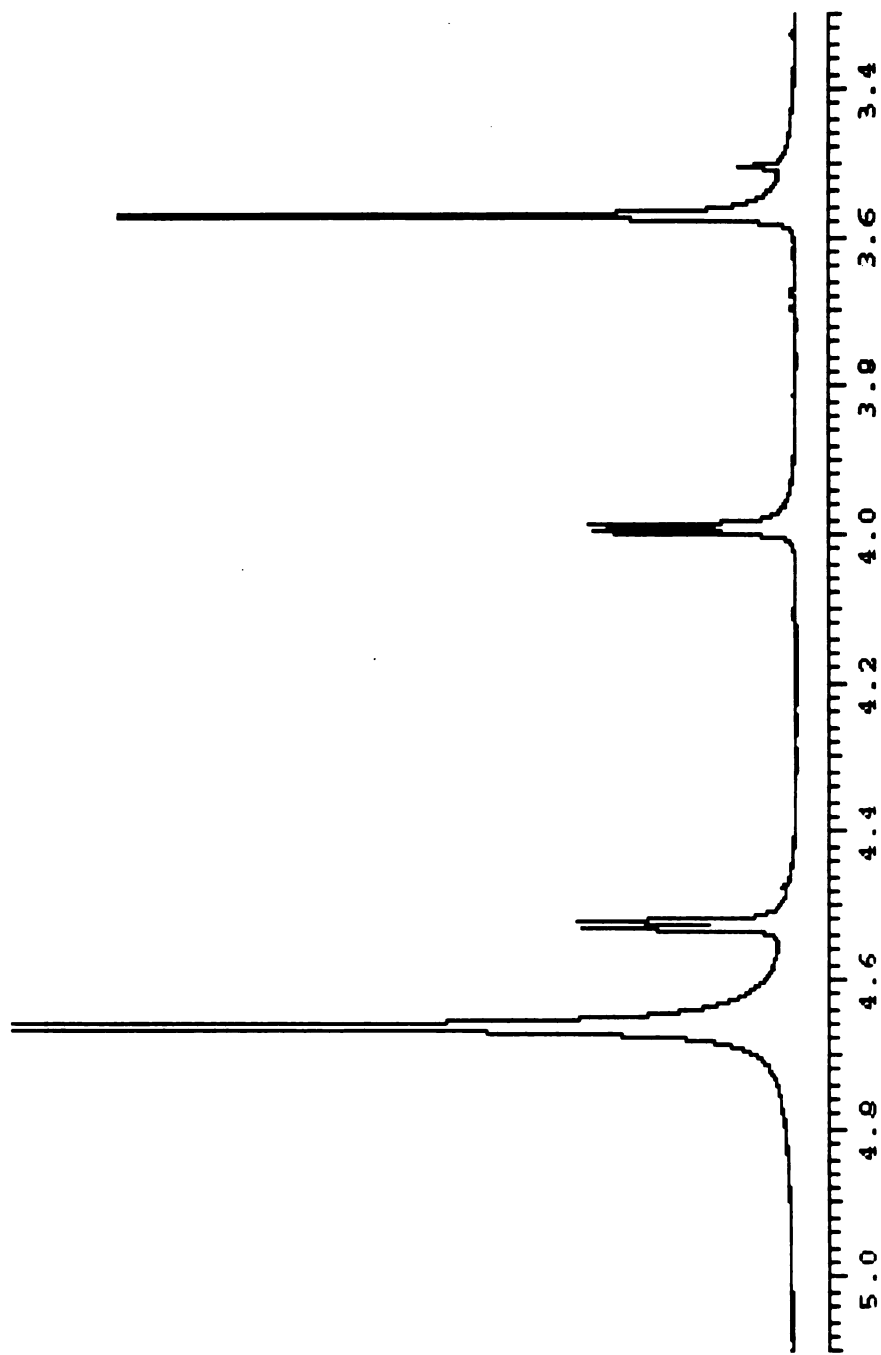
¹H-NMR spectrum of aspartic derivative (2-(1,2-Dicarboxy-ethylamino)-3-hydroxy-succinic acid)

Scheme 2.5 Synthesis of glycine derivative (2-(Carboxymethyl-amino)-3-hydroxy-succinic acid)



Glycine acid (0.85g, 0.01136 moles) in water was titrated with 1 M NaOH to pH 9.6 which corresponds the pK_a of the α -amino group. Epoxysuccinic acid (1.50g, 0.01136 moles) was added, upon which the pH dropped to less than 4. Base was added to raise the pH 9.6. The mixture was heated in an oil bath at 80 °C for 4 hours in a flask attached to a reflux condenser. After allowing the reaction mixture to cool to room temperature, ethanol was added into the solution until two immiscible liquid formed. The supernatant was decanted off and the filtrate was repeatedly washed with ethanol. The amorphous sample was crystallized by titrating it to \approx pH 4 with concentrated HCl. A Buchner filter funnel with medium frit was used to isolate the crystallized product. To remove any impurities such as tartaric acid or epoxysuccinic acid, the amino derivative was washed in methanol. The unreacted amino acid was removed by dissolving the sample in water which resulted in crystallization of the amino acid. After drying, the product was characterized by ¹H NMR in D₂O. Mass Spectrometry analysis was attempted but the results were inconclusive. Consequently, only the NMR was used as the definitive method of choice.

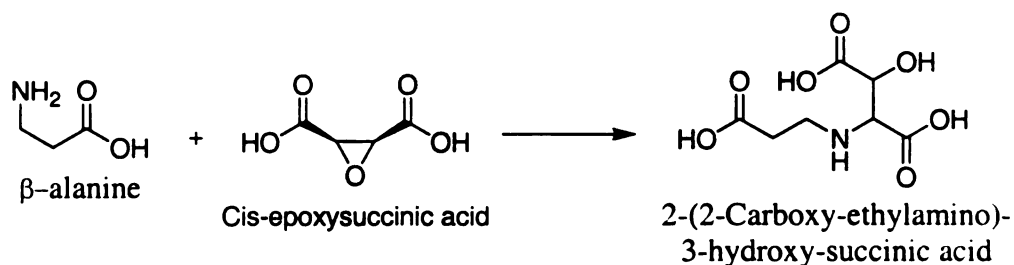
Glycine derivative ¹H-NMR (300 MHz, D₂O @ 25 °C): 3.571 (s, 2H-C(2')); 3.992 (dd, 1H-C(2)); and 4.526 (dd, 1H-C(3)).



Spectrum 2.5

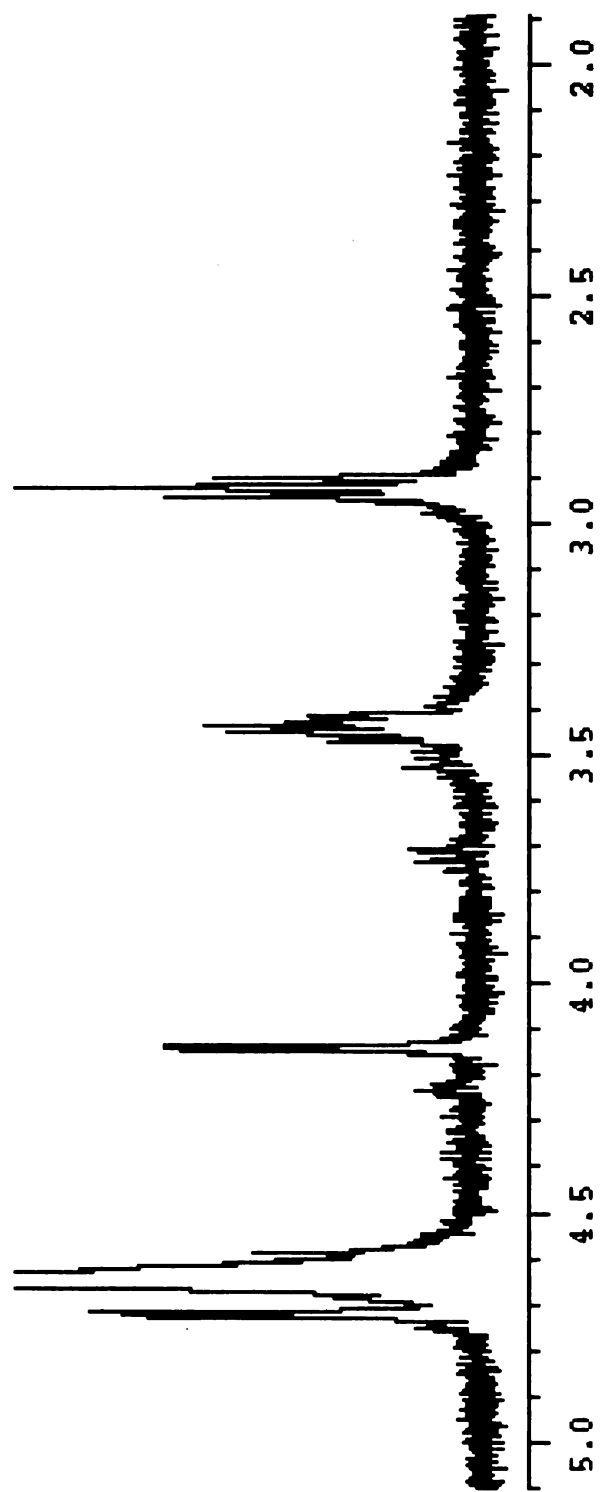
¹H-NMR spectrum of glycine derivative (2-(Carboxymethyl-amino)-3-hydroxy-succinic acid)

Scheme 2.6 Synthesis of β -alanine derivative (2-(2-Carboxy-ethylamino)-3-hydroxy-succinic acid)



β -alanine acid (1.01g, 0.01136 moles) in water was titrated with 1M NaOH to pH 9.7 which corresponds to the pK_a of α -amino group. Epoxysuccinic acid (1.50g, 0.01136 moles) was added, upon which the pH dropped to less than 4. Base was added to raise the pH to 9.7. The mixture was heated in an oil bath at 80 °C for 4 hours in a flask attached to a reflux condenser. After allowing the reaction mixture to cool down to room temperature, ethanol was added into the solution until two immiscible liquids formed. The supernatant was decanted off and the filtrate was repeatedly washed with ethanol. The amorphous sample was crystallized by titrating it to \approx pH 4 with concentrated HCl. A Buchner filter funnel with medium frit was used to isolate the crystallized product. To remove any impurities such as tartaric acid or epoxysuccinic acid, the amino derivative was washed in methanol. The unreacted amino acid was removed by dissolving the sample in water which resulted in crystallization of the amino acid. After drying, the product was characterized by ^1H NMR in D_2O . Mass Spectrometry analysis was attempted but the results were inconclusive. Consequently, only the NMR was used as the definitive method of choice.

β -Alanine derivative ^1H -NMR (300 MHz, D_2O @ 25°C): 2.919 (m, 2H-C(3')); 3.4335 (m, 1H-C(2')); 4.36 (m, 1H-C(2)); and 4.72 (m, 1H-C(3)).



Spectrum 2.6

¹H-NMR spectrum of β -alanine derivative (2-(2-Carboxy-ethylamino)-3-hydroxy-succinic acid)

2.2.1 CALIBRATION CURVE

Calcium chloride dihydrate was purchased from Fisher Scientific and used as received to prepare a stock solution of 0.01M $\text{CaCl}_2 \cdot 2\text{HCl}$ (1000 ppm, hardness CaCO_3) with distilled deionized water and 0.03M NH_4Cl /0.07M NH_4OH buffer (pH=9.5, ionic strength of 0.1M, Columbus Chemical Industries, Inc). Standard solutions ranging from 200 ppm to 10 ppm were prepared by dilution of the stock solution with the buffer. A plot of the logarithm of calcium ion concentration versus the normalized potential was constructed prior to each titration.^{7,8} This calibration was necessary to minimize the effect of signal fluctuations due to solution condition (ionic strength, pH, etc.).

Potentiometric measurements were conducted with a calcium-selective electrode obtained from Orion Research, Inc (model 97-20 ionplus electrode).

2.2.2 TITRATION

The electrode was immersed in 50 mL of 200 ppm CaCO_3 solution at 25°C and the meter reading was taken while the solution was being stirred by magnet.⁹ The calcium binding agent solution was added in small increments and the equilibrium-free calcium ion concentration was measured. When the meter reading indicated less than 10 ppm present in solution, the titration was stopped. The data collected were normalized, and from the calibration curve the concentration of the free calcium ion was obtained

2.2.3 NEPHELOMETRY EXPERIMENT

A SPEX Fluorolog 1681 equipped with a 150 W xenon lamp as the light source and a PMT detector was employed for nephelometry, see figure 1. Light from the excitation spectrophotometer was focused onto the sample. The scattered light from the sample was reflected to the front-face collection port in the sample compartment module and collected by the emission spectrophotometer and directed to the PMT detector. The nucleation and crystal growth was monitored photometrically at 550 nm because this wavelength provided a better scattering signal to noise ratio compared to the other wavelengths. In addition, it is in the region of the xenon lamp output profile that has a flat baseline.

Experiments were performed in a 40 mL quartz cuvette, and the supersaturated solutions were prepared by mixing equal volumes of calcium chloride and sodium citrate stock solutions. The aqueous stock solutions of 5 mM calcium chloride dihydrate and sodium oxalate were buffered at pH 5.5 with 9 mM MES (2-[N-Morpholino] ethanesulfonic acid) and brought to an ionic strength of 0.15M with sodium chloride. The MES has no chelation properties. A pH of 5.5 was chosen because it is the pH value frequently observed in the morning urine of calcium stone-formers.¹⁰ An aliquot of 6 mL of 5 mM calcium chloride solution was transferred in a sample cell followed by 24 mL of 9 mM MES buffered solution. While stirring the sample solution with a Teflon-covered magnetic bar, 6 mL of the 5 mM sodium oxalate solution was added quickly. Readings of the light scattering were recorded every second using a PMT detector. During the inhibition study, 6 mL of 5 mM of the inhibitor was transferred in a sample cell, followed by 6 mL aliquot of 5 mM calcium chloride solution, and 18 mL of the buffered solution.

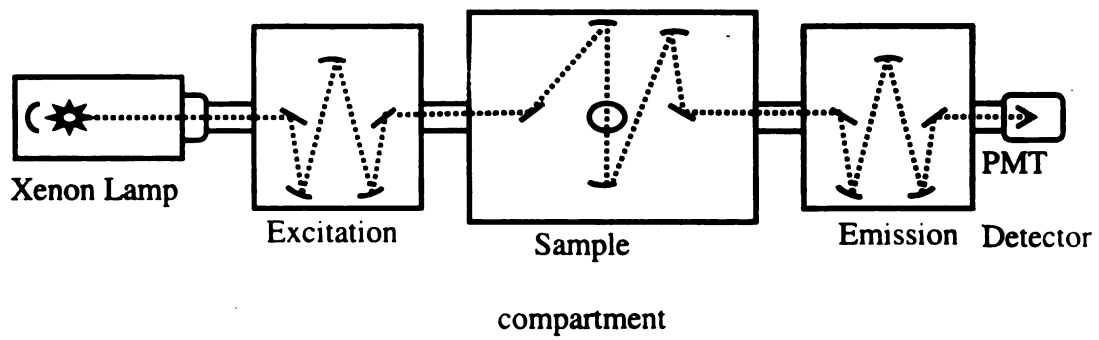


Figure 2.1

Optical Schematic of the spectrometer for nephelometry study

As before, the reactant was added rapidly, and the scattered light intensity readings recorded. Aqueous solution was removed by suction filtration, and the isolated calcium oxalate precipitate was analyzed using Raman.

2.3 RESULTS AND CONCLUSION

2.3.1 CHELATION CONSTANTS

The solution conditions including ionic strength, temperature, and pH and cell variables such as depth of electrode immersion and stirring rate affect the electrode response. The random fluctuation of the cell potential values was corrected by normalization of the data to a ratio. The r^2 regression analysis was determined to be around 0.9984 ± 0.0004 .

Both the samples and the standards were prepared in a similar way which made it possible to determine the quantity of free calcium by reading directly from the calibration curve. The amount of bound calcium (mmol) was calculated by subtracting the free calcium from the total. Figure 2.2 shows that the bound calcium increased as a function of the ligand added. At low ligand concentration, we see a linear relationship between added chelating agent and amount of calcium bound. For the lysine derivative, a deviation from linear curve was observed near the equivalence point, and more so at higher ligand concentrations. The stability constant or chelation constant of 1 to 1 organic chelate with calcium can be written as follows

$$K = \frac{[Ca_2L^{(n-2)-}]}{[Ca^{2+}][L^{n-}]}$$

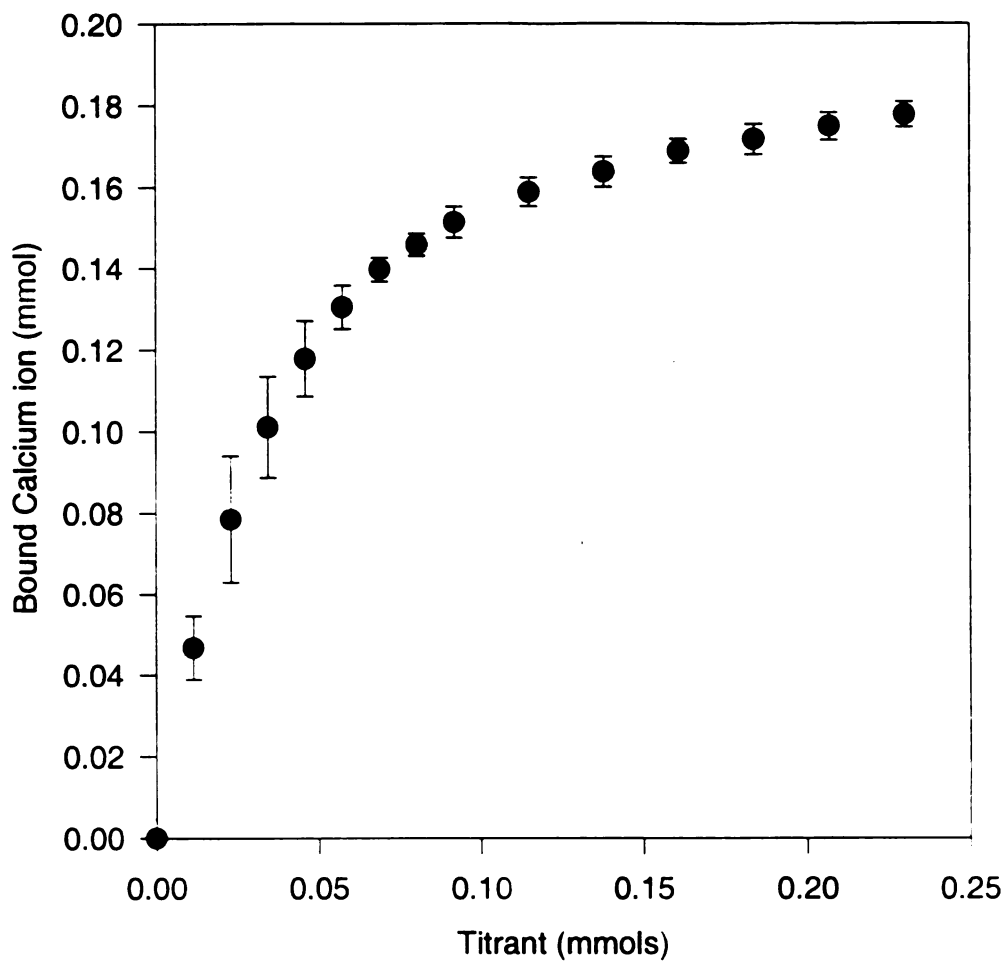


Figure 2.2

A plot of moles of bound Ca^{2+} vs moles of titrant (lysine derivative). Data of bound calcium was from the average of three replicates. Experimental conditions: 200 ppm calcium concentration, 0.03M NH_4Cl /0.07M NH_4OH buffer (pH=9.5, ionic strength of 0.1M NaCl, 25 °C).

where L represents the chelating agent and n is the anionic charge on the chelator. Figure 2.3 shows a plot of $\log K$ versus titrant concentration which has three unique regions. In the region before the equivalence point, the chelation factor increases slowly as a function of titrant concentration. Around the equivalence point, an inflection is observed. The chelation factor after the equivalence point appears to be more constant as a function of titrant. The average chelation factor was obtained by taking the mean average of the chelation factor after the equivalence point. The results have been summarized in table 2.1. EDTA is reported to have a calcium chelation value of about 7.0, which exceeds the chelation strengths of our compounds.¹¹ However, these compounds would make good substitutes for citrate ions because their chelating strengths are statistically similar. According to Crutchfield, an efficient binding agent must have $\log K_{Ca} \geq 5$.¹² Among the compounds studied, only lysine derivative comes close to meeting this criterion.

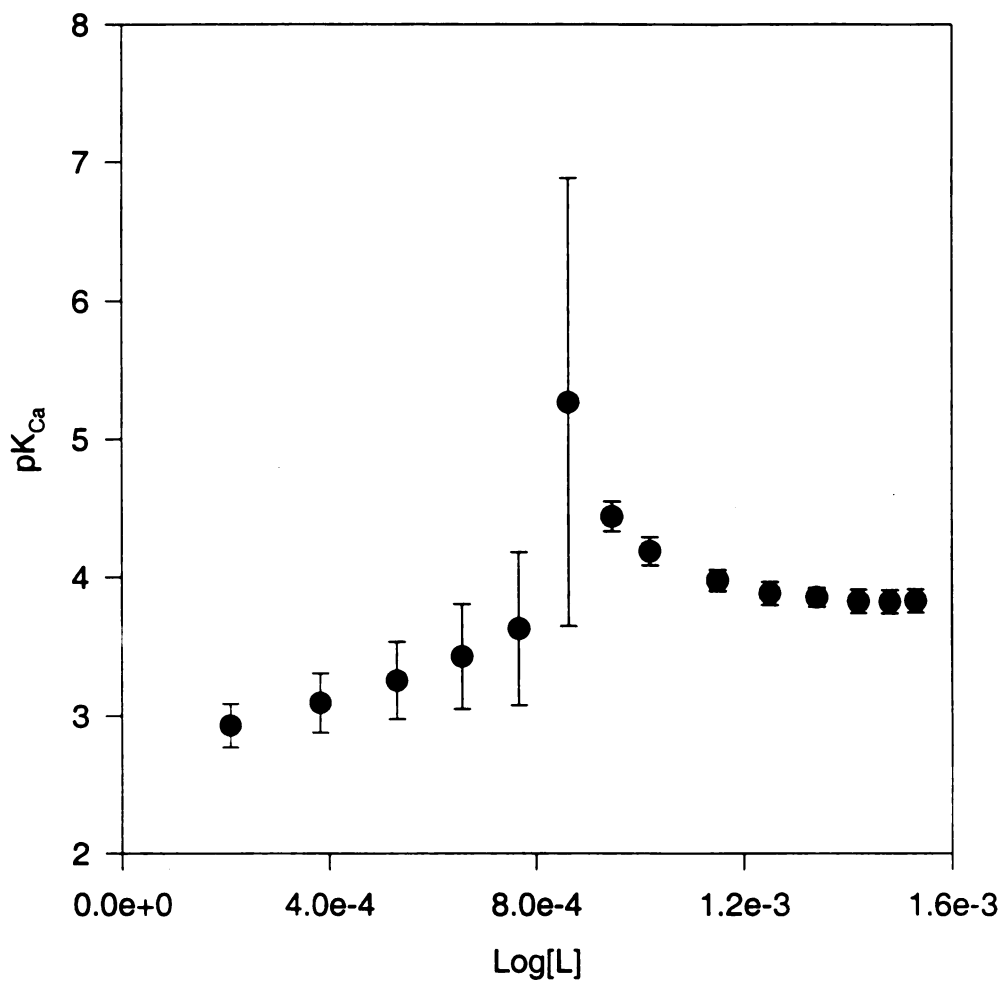


Figure 2.3

pK_{Ca} versus lysine derivative concentration. The pK_{Ca} was determined from the average of three replicates. Experimental conditions: 200 ppm calcium concentration, 0.03M $\text{NH}_4\text{Cl}/0.07\text{M}$ NH_4OH buffer (pH=9.5, ionic strength of 0.1M NaCl, 25 °C).

COMPOUNDS	pK _{Ca}
Citric Acid	3.48 ± 0.40
Glycine derivative	3.60 ± 0.42
β-Alanine derivative	3.41 ± 0.26
Lysine derivative	4.12 ± 0.09
Arginine derivative	3.28 ± 0.18
Aspartic derivative	3.54 ± 0.30
Glutamic derivative	3.61 ± 0.41

Table 2.1

Calcium chelation capacity of amino acid derivatives compared to citrate as determined by calcium-selective electrode (model 97-20 ionplus electrode).

2.3.2 CRYSTALLIZATION KINETICS

Scattered radiant power Φ_{sc} is empirically related to the concentration of suspended particles by the following equation

$$\Phi_{sc} = \Phi_o K_{sc} m \quad (2.1)$$

where K_{sc} is an experimentally obtained constant, Φ_o is the incident radiant power, and m is the mass of studied particle. In nephelometry, the size and shape of the particles have a large effect on the radiant power of scattering.¹³ Hence, nephelometry is an appropriate tool for monitoring nucleation as well as crystal growth. In order to obtain precise and accurate results, factors such as pH, temperature, concentration of reagents, ionic strength, and data acquisition time must be carefully reproduced. Figure 2.4 shows a typical experimental result wherein the amount of particles formed increases with time until a maximum was reached. As new particles are formed and grow, the signal intensity increases. Concurrently, noise signal increases due to multiple light scattering from particles crossing the light path more than once. As a consequence, the Savitsky-Golay algorithm was used to smooth the data from which all the kinetic parameters were recovered.

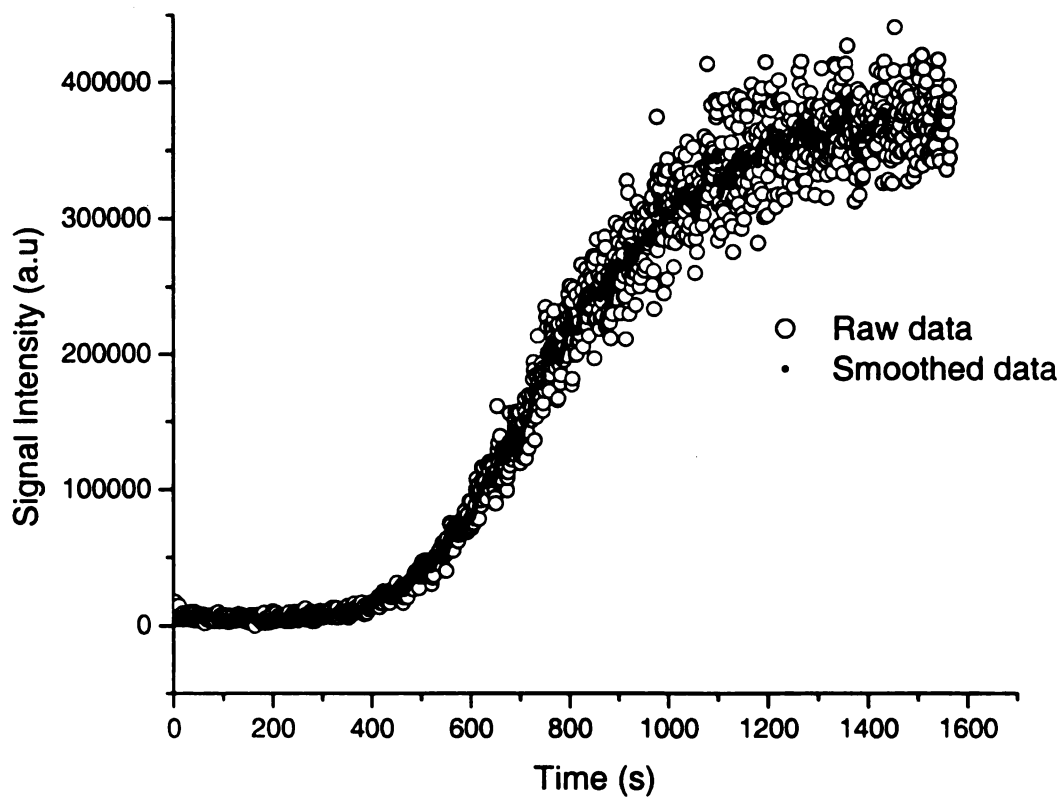


Figure 2.4

Typical curve of calcium oxalate crystallization using nephelometry. Experimental conditions: calcium concentration, 0.8 mM, oxalate concentration, 0.8 mM; T° , 28.0°C; pH 5.5; ionic strength, 0.15M NaCl. The clear line represents the smoothed data using Savitsky-Golay algorithm.

The scattered radiant power is a parameter that corresponds to the particle concentration and increases due to the mass accumulation of the solutes. Thus, supersaturation can be alternatively defined in terms of the radiant power obtained at any other concentration and at the steady state region (i.e. at the end of the experiment), Φ_{sc} and $^*\Phi_{sc}$, respectively. The relative supersaturation is defined by

$$S = 1 - \frac{\Phi_{sc}}{^*\Phi_{sc}} \quad (2.6)$$

Figure 2.5 is a typical desupersaturation curve. The induction period which corresponds to the time between the addition of oxalate and the moment at which a change in optical density is observed was taken as the time corresponding to the intersection of a tangent line with the steepest part of the experimental function with time axis. The length of the induction period can be modulated by impurities which promote or inhibit nucleation. We studied the effect of amino acid derivatives on induction period and the results were compared to t_i in the absence and the presence of citrate. A summary of the induction period for the calcium oxalate crystal growth is summarized in table 2.2. None of the amino acid derivatives significantly prolonged the induction period except the lysine derivative. The inhibition power of lysine derivative on nucleation of calcium oxalate is about 3 times greater than that of citrate, and can prolong the on set of calcium oxalate crystals 5 times longer relative to the control.

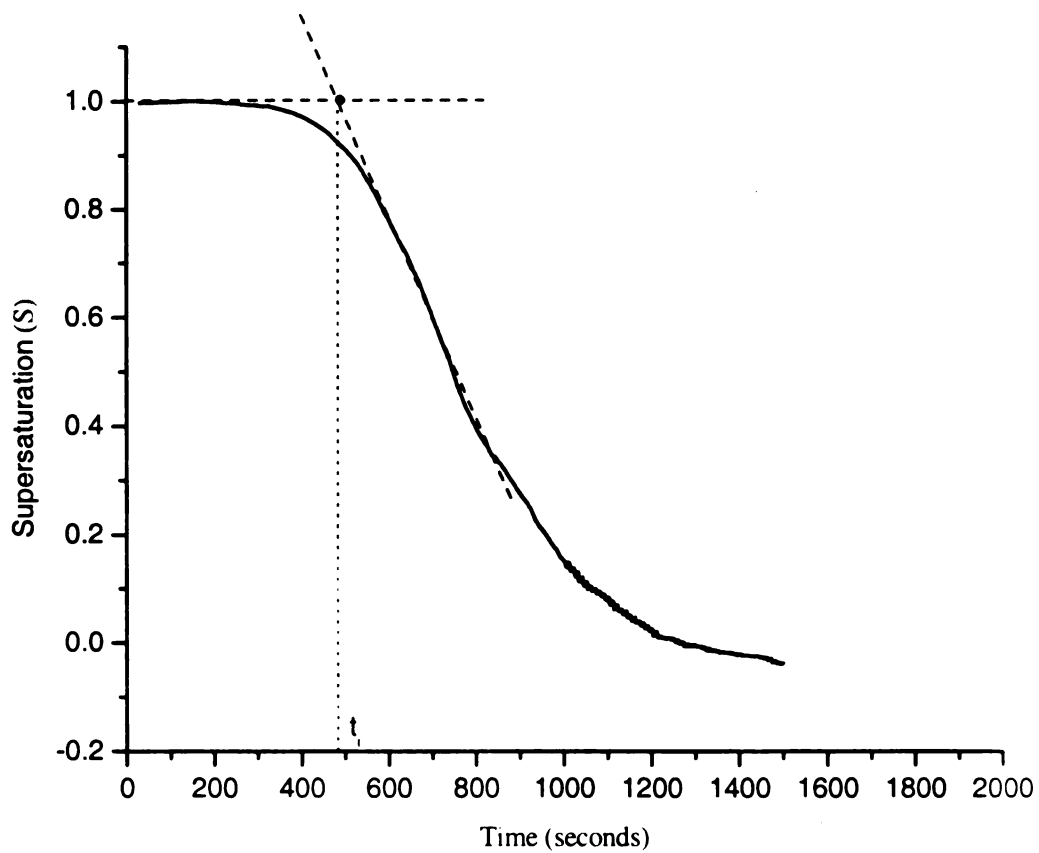


Figure 2.5

A typical desupersaturation curve for the system $\text{CaCl}_3 \cdot 2\text{H}_2\text{O} + \text{Na}_2\text{C}_2\text{O}_4$. Experimental conditions: calcium concentration, 0.8 mM, oxalate concentration, 0.8 mM; T , 28.0°C; pH 5.5; ionic strength, 0.15M NaCl.

Additives	Induction time (s)	Growth Inhibitors
	$t_i \pm 50$	$\%I = (1 - S_i - S_c) \times 100$
Control	340	
Citrate	640	84
Lysine derivative	1800	98
Aspartic derivative	430	
Glutamic derivative	340	
Glycine derivative	460	28
β -alanine derivative	450	11
Arginine derivative	350	41

Table 2.2

Effects of inhibitors on calcium oxalate nucleation and crystal growth.
 Experimental conditions: calcium oxalate, and inhibitor concentrations were all at 0.8 mM, T°, 28.0°C; pH 5.5; ionic strength, 0.15M.

The percentage of inhibition determined from the turbidity slopes of the crystal growth curve in the presence (S_i) and absence (S_c) of additives were calculated as $[1 - (S_i/S_c) \times 100]$.¹⁴ At pH 5.5, the inhibitory effect of the lysine derivative and citric acid with regard to the crystallization of CaC_2O_4 indicated 98% and 84% inhibition, respectively, while the glycine derivative, β -alanine derivative, and arginine derivative inhibition strength was only marginal (see table 2.2). On the other hand, aspartic and glutamic derivative both appear to have no effect on crystal growth.

2.4 CONCLUSION

Nephelometry technique is a fast and simple method to study the inhibitory effect of various substances on calcium oxalate crystal growth. From the induction times alone, it was possible to study nucleation effects, and in addition, we can extract growth kinetic information from the slope of the curve. Lysine derivative by far was the most effective nucleation and growth inhibitor followed by citrate. It is difficult to tell if citrate and lysine derivative exert their inhibitory effect through ion pairing or not. Based on the chelation constant data it does appear that ion sequestration alone does not explain why these compounds make good inhibitors of nucleation and crystal growth. Studying the morphological and phase transformation effect on calcium oxalate crystals is the direction we plan to take next to understand the mechanism of inhibitory effect of the amino acid derivatives and citrate.

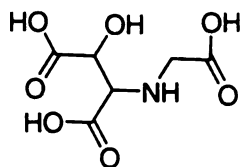
2.5 REFERENCES

- ¹Elsander, A.; Ek, M.; Gellerstedt, G. *Tappi Journal* **2000**, *83*, 73-77.
- ²Watts, R. W. *Journal Of The Royal College Of Physicians Of London* **1973**, *7*, 161-74.
- ³Peacock, M.; Schneider, H.-J. *Urolithiasis : etiology, diagnosis*; Springer-Verlag: Berlin ; New York, 1985.
- ⁴McDonald, M. W.; Stoller, M. L. *Geriatrics* **1997**, *52*, 38-40, 49-52, 55-6.
- ⁵West, E. S.; Todd, W. R. *Textbook of biochemistry*, 3d ed.; Macmillan: New York., 1961.
- ⁶Cerini, C.; Geider, S.; Dussol, B.; Hennequin, C.; Daudon, M.; Veessler, S.; Nitsche, S.; Boistelle, R.; Berthezene, P.; Dupuy, P.; Vazi, A.; Berland, Y.; Dagorn, J. C.; Verdier, J. M. *Kidney International* **1999**, *55*, 1776-86.
- ⁷Rechnitz, G. A.; Lin, Z.-F. *Anal. Chem.* **1968**, *40*, 696-9.
- ⁸Nagarajan, M. K.; Paine, H. L. *JAOCs, J. Am. Oil Chem. Soc.* **1984**, *61*, 1475-8.
- ⁹Blay, J. A.; Ryland, J. H. *Anal. Lett.* **1971**, *4*, 653-63.
- ¹⁰Berg, C.; Tiselius, H. G. *European Urology* **1986**, *12*, 59-61.
- ¹¹Chang, D. M. *JAOCs, J. Am. Oil Chem. Soc.* **1983**, *60*, 618-22.
- ¹²Crutchfield, M. M. *J. Am. Oil Chem. Soc.* **1978**, *55*, 58-65.
- ¹³Ingle, J. D.; Crouch, S. R. *Spectrochemical analysis*; Prentice Hall: Englewood Cliffs, N.J., **1988**.
- ¹⁴Sutor, D. J. *Br. J. Urol.* **1975**, *47*, 585-7.

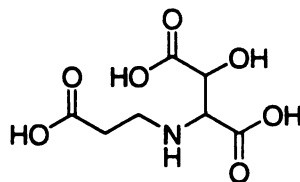
Chapter 3

THE INFLUENCE OF TAILOR-MADE IMPURITIES OF AMINOACID DERIVATIVES ON THE MORPHOLOGY AND PHASE TRANSFORMATION OF CALCIUM OXALATE HYDRATES

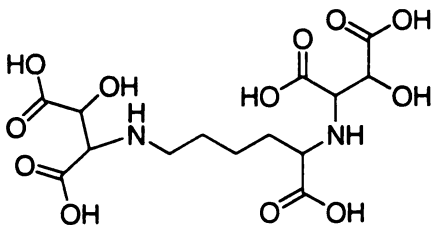
The crystallization of calcium oxalate in the presence of different additives was studied at ambient temperature. Tailor-made amino acid derivatives were used as modifiers and phase transformation modulators. Phase transformation of calcium oxalate in the presence of additives was analyzed by Raman spectroscopy, x-ray powder diffraction (XRD), and environmental scanning electron microscopy (ESEM). All the additives except the glycine and glutamic acid derivatives allowed a phase transformation to take place from a metastable calcium oxalate dihydrate, COD, to the thermodynamically stable monohydrate, COM. The glycine and the glutamic acid derivatives selectively inhibited phase transformation from taking place, while the β -alanine and arginine derivatives converted all COD phase to the COM phase. In all cases, the additives modified the crystal shape of the dihydrate form of calcium oxalate.



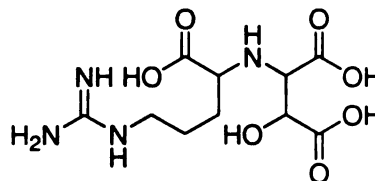
Glycine derivative or
2-(Carboxymethyl-amino)-
3-hydroxy-succinic acid



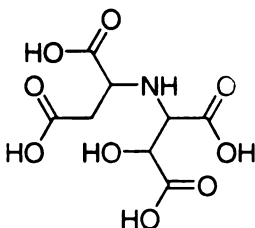
β -Alanine derivative or
2-(2-Carboxy-ethyl-amino)-
3-hydroxy-succinic acid



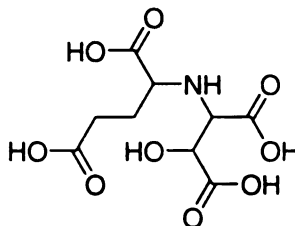
Lysine derivative or
2,6-Bis-(1,2-dicarboxy-2-hydroxy-ethyl-amino)-
hexanoic acid



Arginine derivative or
2-(1-Carboxy-4-guanidino-butyl-amino)-
3-hydroxy-succinic acid



Aspartic derivative or
2-(1,2-Dicarboxy-ethyl-amino)-
3-hydroxy-succinic acid



Glutamic derivative or
2-(1,2-Dicarboxy-2-hydroxy-ethyl-amino)-
pentanedioic acid

Scheme 3.1

Tailor-made additives synthesized by reacting cis-epoxysuccinic acid and amino acid.
See chapter 2 for more details on the synthesis procedure.

3.1 INTRODUCTION

In the pulp and paper industries, calcium oxalate (CaC_2O_4) forms scale deposits on the equipment,¹ while in animals, CaC_2O_4 occurs as a crystalline material in the urinary tract and is the majority constituents in kidney and bladder stones.² Calcium oxalate crystallization results in formation of three types of hydrates: the monohydrate, the dihydrate, and the trihydrate, depending on solution conditions. The monohydrate phase constitutes the main component of the most abundant type of renal calculi that is also the most difficult to treat and the most poorly understood.³ The factors that determine calcium oxalate formation include supersaturation, crystallization kinetics, urinary inhibitors, and epitaxy.^{4,5} In normal urine, the concentration of calcium oxalate is four times higher than its solubility in water.⁶ This high concentration can be attributed to the presence of natural inhibitors, which allows such high calcium oxalate concentration *in vivo*. When the solubility product of calcium oxalate is exceeded, nucleation and crystal growth of calcium oxalate takes place, leading to stone formation.⁷

Treatment of kidney stones has improved dramatically with the introduction of extracorporeal shock wave lithotripsy (ESWL). However, stone prevention is a much less invasive and a more cost-effective approach to patient management. Therefore, calcium oxalate crystallization studies play an important role in urolithiasis research and clinical management. The interest in calcium oxalate crystal growth is oriented to suppress it. Citrate is commonly used as an inhibitor of urinary stone formation,⁸ and works by controlling the average size of calcium oxalate crystals as well as nucleation time, thus it prevents retention in the ducts and the eventual development of kidney

stones.⁹ For healthy patients, it is also thought that calcium and oxalate ions are encapsulated in a protective colloid that keeps the precipitate in colloidal suspension.¹⁰

The important conditions for crystal growth are concentrations of the crystallizing species, the solution temperature, the pH, the ionic strength, and the concentrations growth-modifiers.¹¹ The most important technique used today for influencing crystal growth and the crystallization process is the addition of impurities. In this study we have performed experiments in the presence and absence of tailor-made additives (glycine derivative, β -alanine derivative, lysine derivative, arginine derivative, aspartic derivative, and glutamic derivative), and an additive with biological relevance, citrate. The focus of the study was on the habit modification and phase transformation effects of the additives. We have addressed the synthesis procedure of these compounds elsewhere.¹² Amino acid derivatives (scheme 3.1) were chosen for their opposite nature in steric hindrance, carboxylate composition, and size. There are numerous techniques which can be applied to study the crystal phases. Our method of choice are, Raman spectroscopy (RS), environmental scanning electron microscopy (ESEM), and x-ray powder diffraction (XRD).^{13,14,15,16}

3.2 EXPERIMENTAL METHODS

Experiments were performed in a 250 mL volumetric flask, and the supersaturated solutions were prepared by mixing equal volumes of calcium chloride and sodium nitrate stock solutions. The aqueous stock solutions of 5 mM calcium chloride dihydrate and sodium oxalate were buffered at pH 5.5 with 9 mM MES (2-[N-Morpholino] ethanesulfonic acid) and brought to an ionic strength of 0.15M with sodium chloride. The MES has no chelation properties. A pH of 5.5 was chosen because it is the pH value frequently observed in the morning urine of calcium stone-formers.¹⁷ An aliquot of 25 mL of calcium chloride dihydrate was transferred in a sample cell followed by 25 mL of 9 mM MES buffered solution or 5 mM solutions tailor-made additives prepared in buffered solution. While stirring the sample solution with a teflon-covered magnetic bar, 25 mL of the control solution (sodium oxalate) was added quickly. Once the mixing was done, the magnetic stirrer was stopped to allow the crystals to grow without breakage. Aqueous solution was removed by suction filtration to isolate the crystals, and the Raman spectra of the calcium oxalate precipitate was obtained.

Raman spectra were recorded using a HoloProbe Process Raman Analyzer (Kaiser Optical Systems) equipped with a GaAlAs diode laser. The power of the incident 785 nm laser beam was about 100 mW on the sample's surface. The Raman scattered laser light input signal was collimated, then passed through a notch filter (SuperNotch-Plus™), and focused on the spectrograph entrance slit. The diffracted light from the spectrograph was transmitted to the charge coupled detector (CCD) by a volume holographic transmission grating (HoloPlex™ grating). The CCD chip was 1024x128 EEV MPP with pixel size of 26 μm and an operating temperature set at -40°C.

Photomicrographs of the crystals were obtained with environmental scanning electron microscopy (ESEM). Subsequently, the powder X-ray diffraction analysis was performed on the finely powdered samples with the use of the CuK_α (40 kV and 20 mA) radiation with a scanning speed of $0.03^\circ 2\theta/\text{min}$.

3.3 RESULTS AND DISCUSSIONS

In a crystallization process, where the formation of several phases is possible, the Ostwald-Lussac empirical rule states that the phase with the highest solubility is kinetically favored.¹⁸ The solubility products of calcium oxalate hydrates at room temperature are reported as follows: COT (4.81×10^{-9} moles²/liter²), COD (2.82×10^{-9} moles²/liter²), and COM (2.00×10^{-9} moles²/liter²).^{19, 20, 21} Since impurities have great influence on crystal size, shape, and purity,²² we investigated the selective effect of the additives on the habit modification and the phase transformation of CaC_2O_4 using Raman spectroscopy, x-ray powder diffraction, and environmental scanning electron microscopy.

The characteristic Raman bands due to the C=O symmetric stretching are observed around 1463 cm^{-1} for the COM and at 1473 cm^{-1} in the case of COD.²³ When the crystallized samples were left in solution for about an hour, then the supernatant was decanted off. Raman spectra of the wet crystalline material was obtained, and only the dihydrate form of calcium oxalate was detected as shown in figure 3.1a. Whereas the Raman spectra of calcium oxalate crystals left in aqueous solution for 24 hours in the presence of tailor-made additives, confirmed that a change in phase took place except for the samples crystallized in the presence of the glycine and glutamic derivatives. Figure 3.1b indicates the presence of the COM and the COD in different proportions for the

control sample as well as samples crystallized in the presence of the additives. The Raman spectra indicate that the crystals grown in the presence of these tailor additives: β – alanine and arginine derivatives transformed completely from the COD crystal phase to the COM crystal phase after 24 hours.

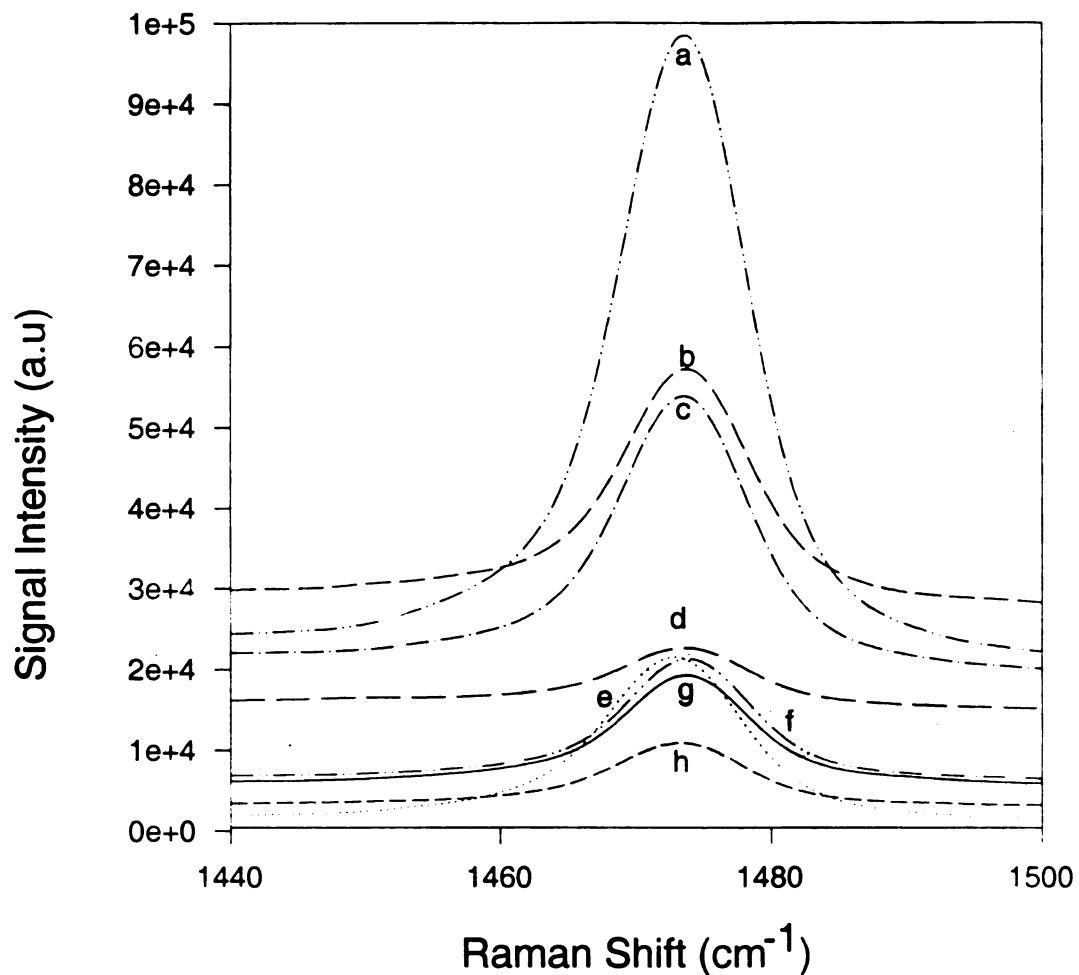


Figure 3.1a

Raman spectra of calcium oxalate hydrates after 1 hour in solution. a) alanine derivative, b) glycine derivative, c) arginine derivative, d) citrate, e) glutamic derivative, f) control, g) lysine derivative, h) aspartic derivative Experimental conditions: calcium concentration, 0.8 mM, oxalate concentration, 0.8 mM; T° , 28.0°C; pH 5.5; ionic strength, 0.15M NaCl. Concentration of additives, 0.8mM.

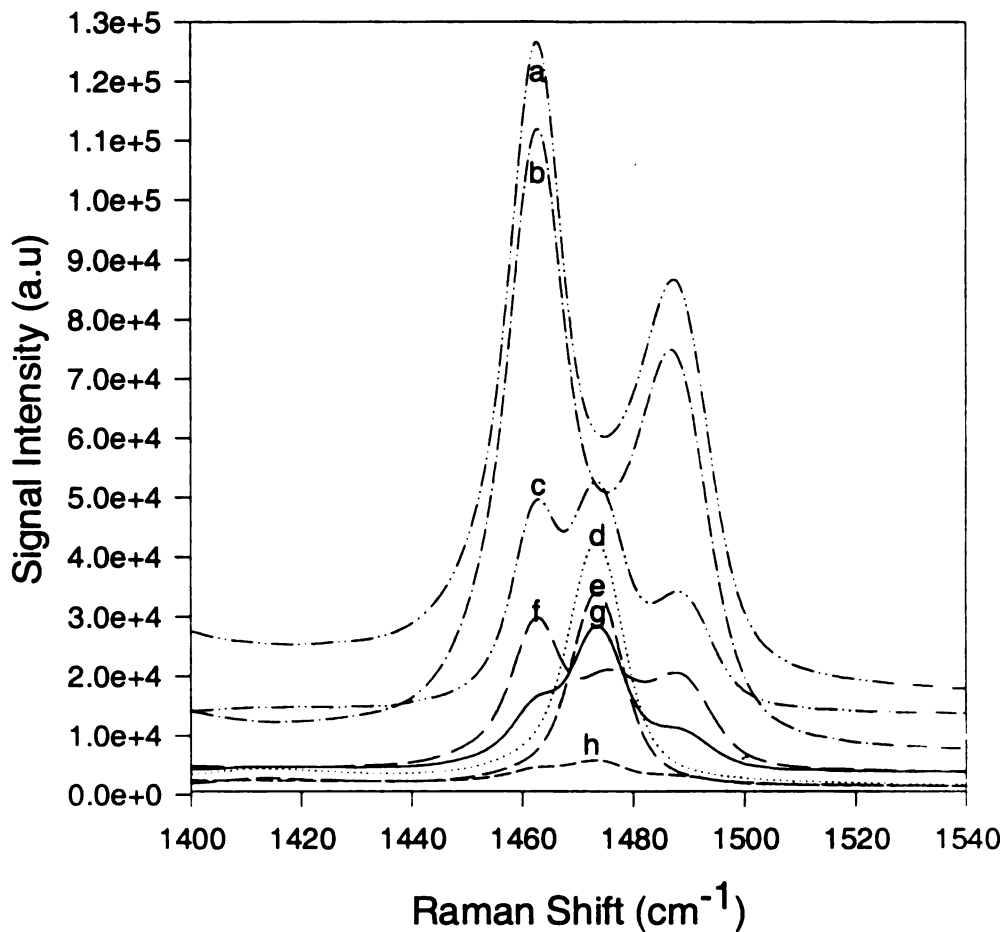


Figure 3.1b

Raman spectra of calcium oxalate hydrates after 24 hours in solution. a) alanine derivative, b) arginine derivative, c) control, d) glutamic derivative, e) glycine derivative, f) citrate, g) lysine derivative, h) aspartic derivative. Experimental conditions: calcium concentration, 0.8 mM, oxalate concentration, 0.8 mM; T°, 28.0°C; pH 5.5; ionic strength, 0.15M NaCl. Concentration of additives, 0.8mM.

The morphology of calcium oxalate hydrates were observed by ESEM. Figure 3.2 is a typical micrograph for COD prepared without additives. The crystal shape is tetrahedron. In the presence of tailor-made additives, some of the crystal faces were modified. Figures 3.3A-3.4D are micrographs of COD crystals which were crystallized in the presence of glycine, β -alanine, glutamic, and arginine derivatives. The crystal faces appear to have been modified from the typical tetrahedron shape to a needle-like shape. As for samples crystallized in the presence citrate, we see a change in all the crystal faces for the crystals affected as shown in figure 3.5. However, the crystal shape appears more plate-like.

When the crystallization of calcium oxalate was allowed to take place in solution for 24 hours in the presence and absence of additives, several interesting results were obtained. Phase transformation from the COD to COM took place in all cases except samples crystallized in the presence of glutamic and glycine derivatives. These additives prevented any phase transformation from taking place as shown in figure 3.6. Interestingly, only the crystals grown in the presence of the glutamic derivative preserved the original crystal habit of COD. On the other hand, the glycine derivative allowed habit modification to take place from the needle-like shape to the tetrahedron like shape. Figure 3.3a and 3.7 indicates the effect of glycine derivative on the crystal shape after an hour, and 24 hours in solution respectively. The β -alanine and arginine derivative allowed complete phase transformation to take place from the COD to the thermodynamically stable COM.

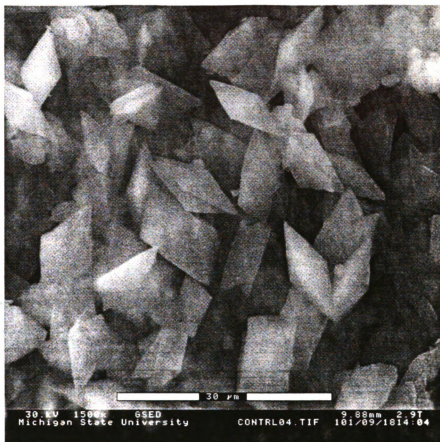


Figure 3.2

ESEM of a typical COD morphology. Experimental conditions: calcium concentration, 0.8 mM, oxalate concentration, 0.8 mM; T° , 28.0°C; pH 5.5; ionic strength, 0.15M NaCl.

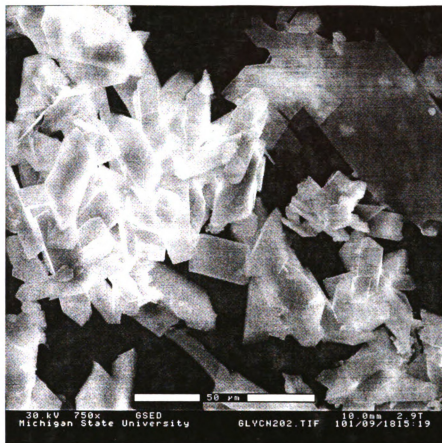


Figure 3.3a

ESEM of COD formed in the presence of 0.8 mM glycine derivative after left insoluble for 1 hour. Experimental conditions: calcium concentration, 0.8 mM, oxalate concentration, 0.8 mM; T° , 28.0°C; pH 5.5; ionic strength, 0.15M NaCl.



Figure 3.3b

ESEM of COD formed in the presence of 0.8 mM β -alanine derivative after left insolution for 1 hour. Experimental conditions: calcium concentration, 0.8 mM; oxalate concentration, 0.8 mM; T° , 28.0 $^{\circ}$ C; pH 5.5; ionic strength, 0.15M NaCl.



Figure 3.3c

ESEM of COD formed in the presence of 0.8 mM glutamic derivative after left insoluble for 1 hour. Experimental conditions: calcium concentration, 0.8 mM; oxalate concentration, 0.8 mM; T° , 28.0°C; pH 5.5; ionic strength, 0.15M NaCl.

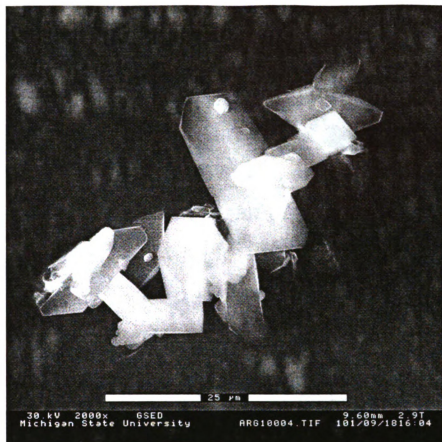


Figure 3.3d

ESEM of COD formed in the presence of 0.8 mM arginine derivative after left in solution for 1 hour. Experimental conditions: calcium concentration, 0.8 mM; oxalate concentration, 0.8 mM; T° , 28.0°C; pH 5.5; ionic strength, 0.15M NaCl.

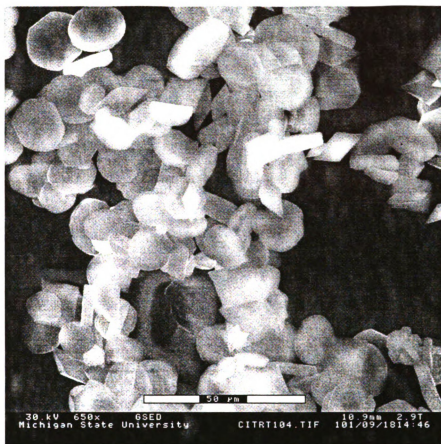


Figure 3.4

ESEM of COD formed in the presence of 0.8 mM citrate after left in solution for 1 hour. Experimental conditions: calcium concentration, 0.8 mM, oxalate concentration 0.8 mM; T° , 28.0°C; pH 5.5; ionic strength, 0.15M NaCl.



Figure 3.5

ESEM of COD formed in the presence of 0.8 mM glutamic derivative after left in solution for 24 hours. Experimental conditions: calcium concentration, 0.8 mM, oxalate concentration, 0.8 mM; T: 28.0°C; pH 5.5; ionic strength, 0.15M NaCl.

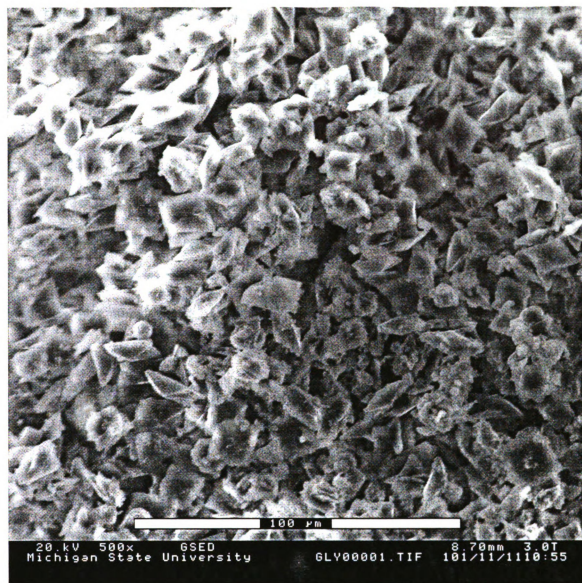


Figure 3.6

ESEM of COD formed in the presence of 0.8 mM glycine derivative after left in solution for 24 hours. Experimental conditions: calcium concentration, 0.8 mM; oxalate concentration, 0.8 mM; T , 28.0°C; pH 5.5; ionic strength, 0.15M NaCl.

The ESEM image shown in figures 3.8 and 3.9 indicates a typical morphology of COM. As for the crystals obtained in the presence and absence of the following additives (lysine derivative, aspartic derivative, and citrate), the ESEM image revealed a mixture COD and COM crystals. See figures 3.10A-3.10D. The COM crystals are much smaller in size compared to the COD.

Powder XRD was used to confirm the morphology of calcium oxalate crystals prepared in the presence and absence of additives. The XRD characteristic reflections of COD crystals which were crystallized for an hour in the presence of the following additives: glycine derivative, β – alanine derivative, arginine derivative, glutamic derivative, and aspartic derivative, confirmed the ESEM image that the morphology faces of the crystallized COD are similar. Figure 3.11 shows the XRD spectra of COD crystals in the absence and presence of citrate and the lysine derivative. The patterns falling at the following position (14.7, 24.3, 10.1, 38.2 and 40.6) in terms of 2θ , had similar peaks; however, not all the peaks were common in the diffractograms. This is not surprising because the ESEM data for these samples indicate that the sample crystallized in the presence of citrate resulted in modified faces, while lysine derivative gave mixtures of products with different crystal habit. Consequently, the diffractograms reflect a mixture of x-ray diffraction pattern resulting from all the crystal faces.

The XRD of the crystals isolated after 24 hours in the presence of β – alanine and the arginine derivative, confirmed that a complete phase transformation from COD to COM took place. From the XRD data shown in figure 3.12, it appears that the glycine derivative modified the COD crystal face because the characteristic reflections of the

crystal faces for the control COD crystal does not match that of the COD crystallized in the presence of glycine derivative.

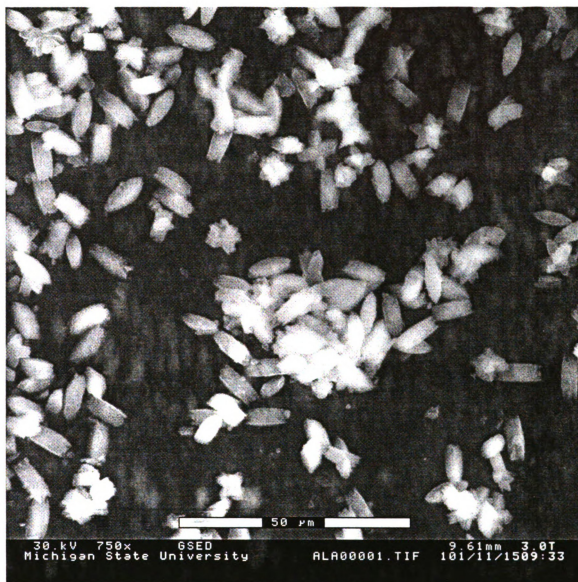


Figure 3.7

ESEM of COD formed in the presence of 0.8 mM alanine derivative after left in solution for 24 hours. Experimental conditions: calcium concentration, 0.8 mM; oxalate concentration, 0.8 mM; T^0 , 28.0°C; pH 5.5; ionic strength, 0.15M NaCl.

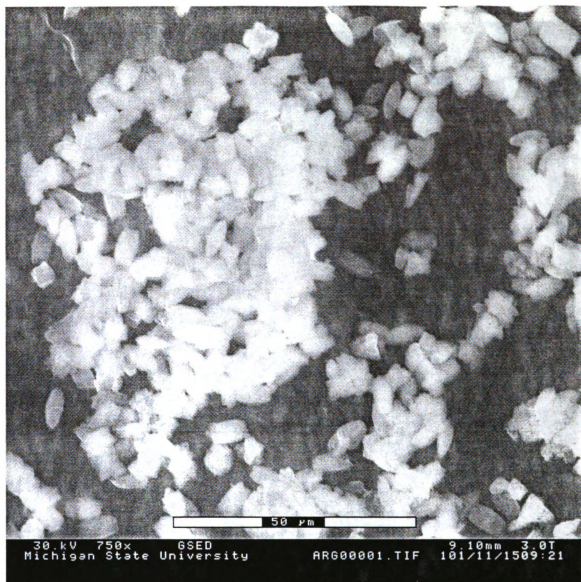


Figure 3.8

ESEM of COD formed in the presence of 0.8 mM arginine derivative after left in solution for 24 hours. Experimental conditions: calcium concentration, 0.8 mM, oxalate concentration, 0.8 mM; T° , 28.0°C; pH 5.5; ionic strength, 0.15M NaCl.

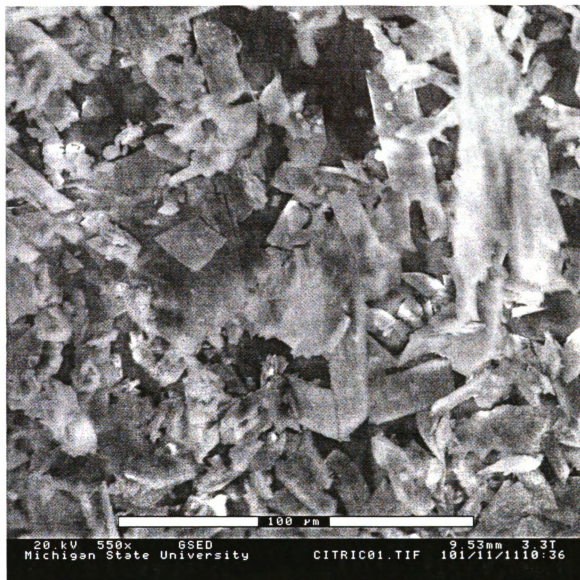


Figure 3.9a

ESEM of COD formed in the presence of 0.8 mM citrate derivative after left in solution for 24 hours. Experimental conditions: calcium concentration, 0.8 mM, oxalate concentration, 0.8 mM; T° , 28.0 $^{\circ}$ C; pH 5.5; ionic strength, 0.15M NaCl.



Figure 3.9b

ESEM of COD formed in the presence of 0.8 mM lysine derivative after left in solution for 24 hours. Experimental conditions: calcium concentration, 0.8 mM, oxalate concentration, 0.8 mM; T° , 28.0°C; pH 5.5; ionic strength, 0.15M NaCl.



Figure 3.9C

ESEM of COD formed in the absence of additives after left in solution for 24 hours.
Experimental conditions: calcium concentration, 0.8 mM, oxalate concentration, 0.8 mM;
 T° , 28.0°C; pH 5.5; ionic strength, 0.15M NaCl.



Figure 3.9d

ESEM of COD formed in the presence of 0.8 mM aspartic derivative after left in solution for 24 hours. Experimental conditions: calcium concentration, 0.8 mM; oxalate concentration, 0.8 mM; T° , 28.0 $^{\circ}$ C; pH 5.5; ionic strength, 0.15M NaCl.

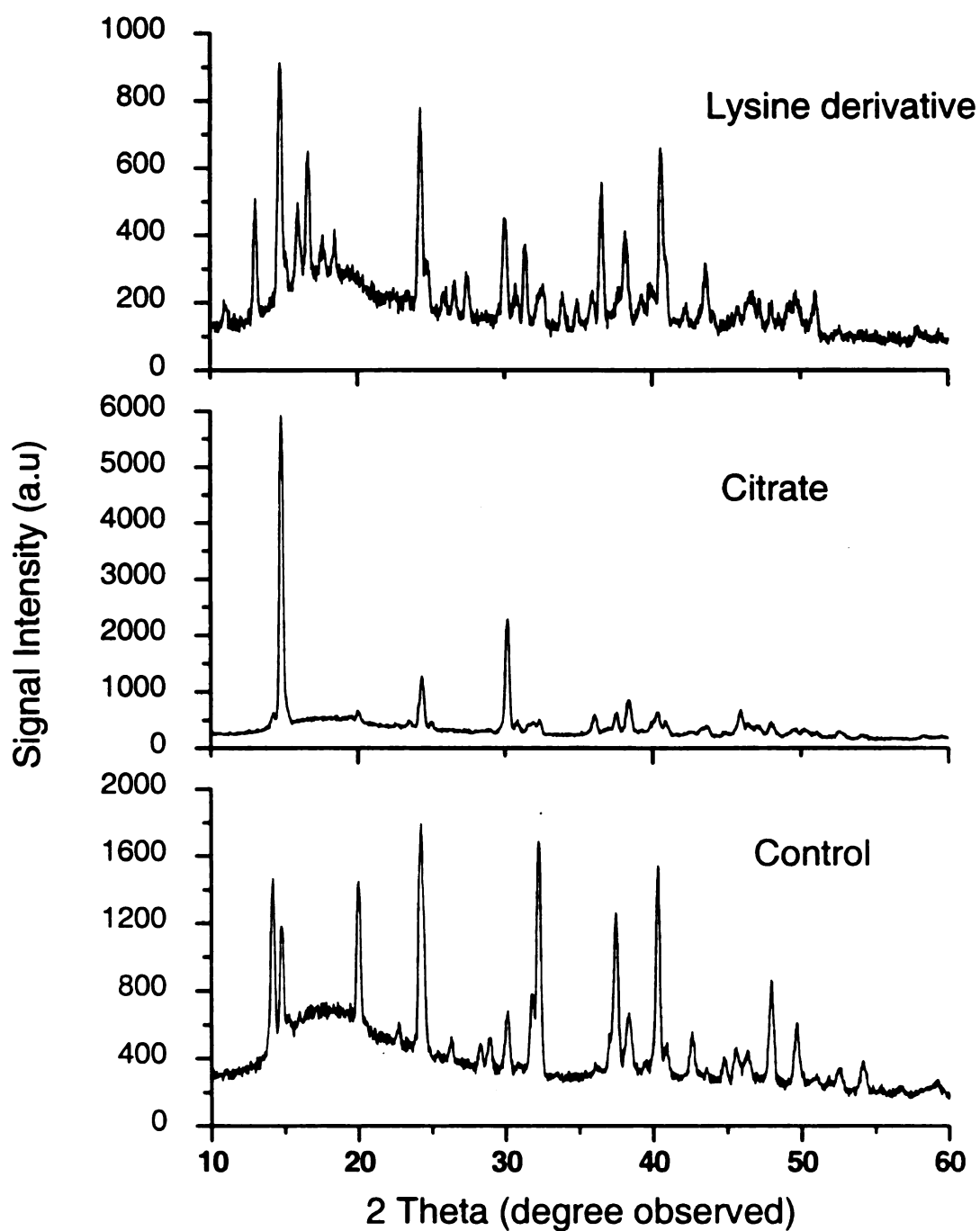


Figure 3.10

XRD spectra of COD crystal of the control sample, and the samples formed in the presence of lysine derivative, and citrate after left in solution for an hour. Experimental conditions: calcium concentration, 0.8 mM, oxalate concentration, 0.8 mM; T: 28.0°C; pH 5.5; ionic strength, 0.15M NaCl.

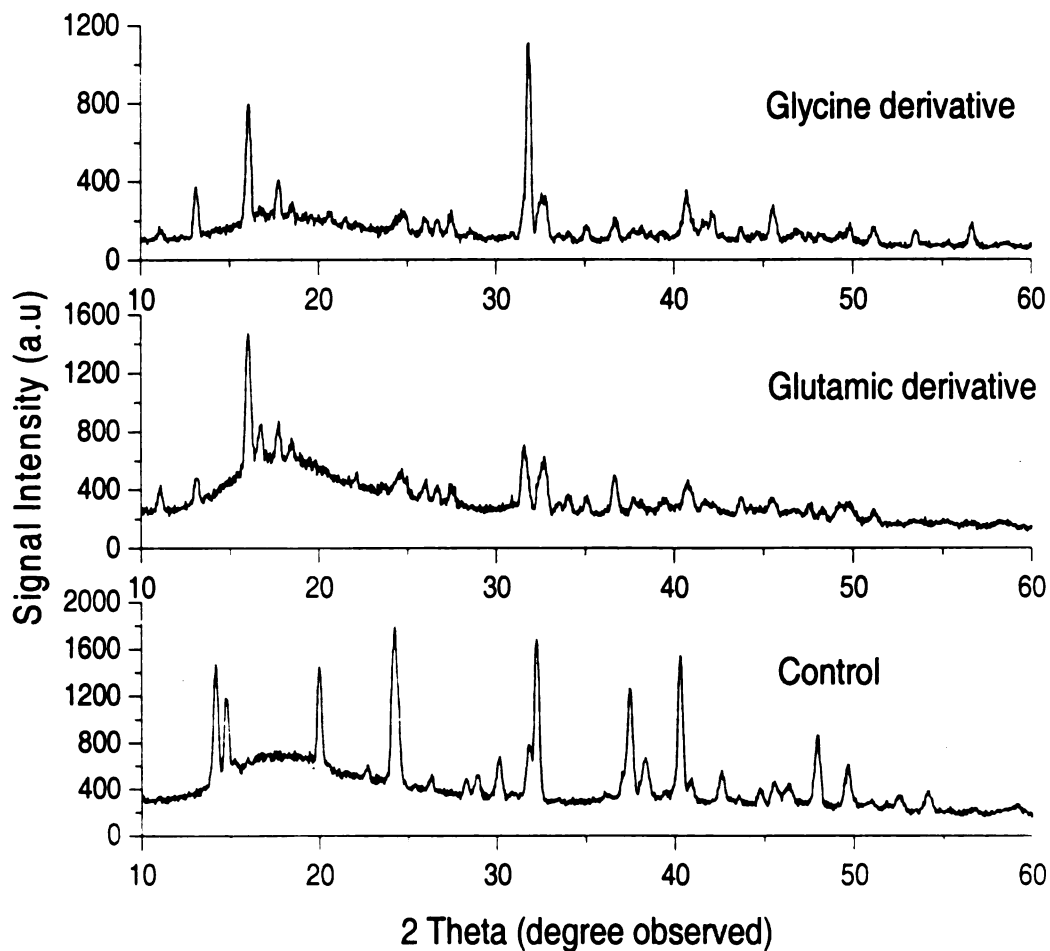


Figure 3.11

XRD spectra of COD crystal of the control sample, and the samples formed in the presence of additives (glutamic and glycine derivative) which prevented phase transformation of COD crystals after it was left in solution for 24 hours. Experimental conditions: calcium concentration, 0.8 mM, oxalate concentration, 0.8 mM; T° , 28.0 $^{\circ}$ C; pH 5.5; ionic strength, 0.15M NaCl.

3.4 CONCLUSION

In this study, we used tailor-made additives, which preferentially influenced specific crystal faces. The observed habit of crystals grown from solutions was unpredictable. No formation of calcium oxalate trihydrate was observed. All the additives modified the crystal habit of the COD in a similar manner. Some of these additives behaved either as phase transformation inhibitors or as promoters. There are two possible explanations for the observed phenomena: surface adsorption, and/or lattice incorporation. Regardless of how the additives influenced the crystallization process, habit modification as well as phase transformation of the calcium oxalate crystal hydrates was expressed quite well. However, we can rule out lattice insertion because these molecules are much bigger in size compared to the oxalate molecule. In addition, the XRD data showed no evidence of diffraction patterns completely different from that of the control sample.

The interpretation of the morphological results based on preferential adsorption of the additives has some legitimacy. We tend to believe that the morphological modification observed is mainly driven by electrostatic interactions of the additives with either oxalate ions and/or calcium ions. It has been reported that surfactants control morphological and phase changes in calcium oxalate crystals through preferential adsorption.^{24, 25} Similar results have been reported for other organic molecules with high negative charge density, such as di- and tricarboxylic acids.²⁶ Although further investigation is needed to prove this, it is safe to say that some sort of specific interaction is taking place with the surface of the calcium oxalate crystal faces.

3.5 REFERENCES

- ¹Elsander, A.; Ek, M.; Gellerstedt, G. *Tappi Journal* **2000**, 83, 73-77.
- ²Watts, R. W. *Journal Of The Royal College Of Physicians Of London* **1973**, 7, 161-74.
- ³Resnick, M. I. *Urolithiasis*; W.B. Saunders: Philadelphia, **2000**.
- ⁴McDonald, M. W.; Stoller, M. L. *Geriatrics* **1997**, 52, 38-40, 49-52, 55-6.
- ⁵West, E. S.; Todd, W. R. *Textbook of biochemistry*, 3d ed.; Macmillan: New York., **1961**.
- ⁶Coe, F. L.; Parks, J. H. *Hospital Practice (Office Edition)* **1988**, 23, 185-9, 193-5, 199-200.
- ⁷Cerini, C.; Geider, S.; Dussol, B.; Hennequin, C.; Daudon, M.; Veessler, S.; Nitsche, S.; Boistelle, R.; Berthezene, P.; Dupuy, P.; Vazi, A.; Berland, Y.; Dagorn, J. C.; Verdier, J. M. *KIDNEY INTERNATIONAL* **1999**, 55, 1776-86.
- ⁸Harrison, T. R. *Principles of internal medicine*, 4th ed.; Blakiston Division McGraw-Hill: New York., **1962**.
- ⁹Chaplin, A. J. *Journal Of Clinical Pathology* **1977**, 30, 800-11.
- ¹⁰J. Butt, *J. Urol.* **1952**, 67, 450.
- ¹¹Finlayson, B. *Kidney International* **1978**, 13, 344-60.
- ¹²C.O. Ngowe and K.A. Berglund, see chapter 2.
- ¹³Byrn, S. R.; Gray, G.; Pfeiffer, R. R.; Frye, J. J. *Pharm. Sci.* **1985**, 74, 565-8.
- ¹⁴Stout, G. H.; Jensen, L. H. *X-ray structure determination; a practical guide*; Macmillan: New York, **1968**.
- ¹⁵Curtin, D. Y.; Byrn, S. R. *J. Amer. Chem. Soc.* **1969**, 91, 6102-6..
- ¹⁶Kontoyannis, C. G.; Bouropoulos, N. C.; Koutsoukos, P. G. *Appl. Spectrosc.* **1997**, 51, 1205-1209.
- ¹⁷Berg, C.; Tiselius, H. G. *European Urology* **1986**, 12, 59-61.
- ¹⁸Ostwald, W. *Phys. Chem.* **1897**, 22, 289-330.

- ¹⁹Nancollas, G. H.; Gardner, G. L. *J. Cryst. Growth* **1974**, *21*, 267-76.
- ²⁰Babic-Ivancic, V.; Fueredi-Milhofer, H.; Purgaric, B.; Brnicevic, N.; Despotovic, Z. *J. Cryst. Growth* **1985**, *71*, 655-63.
- ²¹Tomazic, B.; Nancollas, G. H. *J. Cryst. Growth* **1979**, *46*, 355-61.
- ²²Myerson, A. S. *Handbook of industrial crystallization*; Butterworth-Heinemann: Boston, **1993**. Chapter 3.
- ²³Shippey, T. A. *J. Mol. Struct.* **1980**, *65*, 61-70.
- ²⁴Addadi, L.; Berkovitch-Yellin, Z.; Weissbuch, I.; Van Mil, J.; Shimon, L. J. W.; Lahav, M.; Leiserowitz, L. *Angew. Chem.* **1985**, *97*, 476-96.
- ²⁵Tunik, L.; Addadi, L.; Garti, N.; Fueredi-Milhofer, H. *J. Cryst. Growth* **1996**, *167*, 748-755.
- ²⁶Cody, A. M.; Cody, R. D. *J. Cryst. Growth* **1994**, *135*, 235-45.

FUTURE STUDIES

4.1 INTRODUCTION

The research conducted in chapters 1 and 2 involved the use of a batch crystallization technique in investigations of the crystallization of calcium oxalate. This technique involved the use of a glass beaker or flask, into which the calcium and oxalate solutions are added all at once and the combined solutions were mixed using a magnetic stirrer. The crystallization was initiated spontaneously. As the crystals grew, calcium and oxalate ions disappeared from solution decreasing the relative supersaturation driving force. A crystallization rate was measured by nephelometry. Since the relative supersaturation falls throughout the experiment, the measured rate or the morphology of the crystals is not characteristic of any one value of relative supersaturation. It is important to know that the manner and time scale over which the supersaturation is brought about will affect the different crystallization processes in different ways, the crystal size distribution, crystal phase and habit modification.¹

The prediction and control of the growth habit of crystals are utmost importance for chemical, petrochemical, food, environmental, and pharmaceutical industries. In chapter 1, it was demonstrated how tailor-made amino acid derivatives can be used as modifiers and phase transformation modulators. The two additives from the aliphatic group (glycine and β -alanine derivative) both modified the crystal shape of calcium oxalate, however only the glycine derivative prevented phase transformation from taking place. The basic amino acids used (lysine and arginine derivative) allowed habit modification and phase transformation of calcium oxalate hydrates to take place. It was also demonstrated how derivatives of acidic amino acids (aspartic and glutamic

derivative) affected the crystallization of calcium oxalate hydrate. The glutamic derivative behaved as an inhibitor of phase transformation while aspartic derivative promoted it. In addition, they both promoted habit modification. We learned from chapter 2 that the most effective inhibitor of both nucleation and crystal growth was the lysine derivative, leading to an inhibition of 98%, followed by the citric acid. However, the aliphatic amino acids and the basic amino acid derivatives inhibited less than 50% crystal growth.

Although the lysine derivative appears to be a promising compound which could be used for controlling kidney stones, it still requires more studies to be conducted. It is generally believed that a supersaturation decay method such as batch crystallization does not represent the conditions within the kidney. In order to mimic the physiological condition for the purpose of evaluating inhibitors, constant composition method is the technique of choice.

4.2 PROPOSED STUDIES

4.2.1 CONSTANT COMPOSITION METHOD

The constant composition method used in the measurement of calcium oxalate crystal growth rates was developed by Sheehan and Nancollas.² This method represents the condition within the kidney compared to the supersaturation decay method.³ Calcium and oxalate solutions and crystal seeds are added to a stirred crystallization vessel at the beginning of the experiment and concentrated calcium and oxalate solutions are titrated into the vessel throughout the experiment. Instead of following the depletion of an ion from solution, the amounts of concentrated calcium and oxalate solutions titrated to maintain a constant supersaturation during crystallization are recorded. The calcium

concentration is monitored using a calcium-specific electrode, with the measurement of oxalate with the assumption of equimolar co-precipitation of the oxalate ion. The constant composition method allows for the measurement of crystal growth rates at constant solution conditions, particularly constant supersaturation. Using this method to test the six inhibitors synthesized would give a better insight on their potentials as modifiers, and inhibitors of crystal growth and phase transformation.

4.2.2 SYNTHESIS OF AMINO ACID DERIVATIVES

Only 6 of the 20 amino acids were derivatized. An attempt to derivatize the rest of the amino acid was successful, but limited by the purification process of the product. The synthesis procedure for making the following amino acid derivatives (valine, leucine, isoleucine, methionine, serine, threonine, cysteine, asparagines, and glutamine) involved adding equimolar amount of starting reagents (amino acid and cis-epoxysuccinic acid) and raising the pH of the solution to the pKa value of the amino acid. The unwanted side reaction was formation of tartaric acid was unavoidable. The purification procedure that was devised for aspartic and glutamic derivative did not work well for the other amino acids. A better synthetic route which avoids formation of tartaric acid would be of great interest. Secondly, vigorous testing of these inhibitors as potential therapeutic agents for prevention and/or treatment of urolithiasis.

4.3 REFERENCES

- ¹ Mullin, J. W. *Crystallization*, 3rd ed.; Butterworth-Heinemann: Oxford ; Boston, **1993**.
- ² Sheehan, M. E.; Nancollas, G. H. *Invest. Urol.* **1980**, *17*, 446-50.
- ³ Khan, S. R. *Calcium oxalate in biological systems*; CRC Press: Boca Raton, Fla., 1995.

CONCLUSION

SYNTHESIS AND CHARACTERIZATION OF TAILOR-MADE ADDITIVES FOR INHIBITION OF SPARINGLY SOLUBLE CALCIUM SALT CRYSTALLIZATION

The control of crystals and the crystallization process from solutions using a structurally similar or tailor-made additives has been demonstrated. Our original goal was to inhibit calcium oxalate crystal growth using the amino acid derivatives. To our surprise, only lysine derivative was an effective inhibitor of both nucleation and crystal growth. Since calcium oxalate exist in more than one phase, we then focused our attention on the effect of the amino acid derivatives on the phase transformations of calcium oxalate hydrates. Glycine and glutamic derivatives selectively inhibited phase transformation from taking place, while alanine and arginine derivative promoted phase transformation. The only common effect that was observed in the amino acid derivatives is their ability to modify the crystal faces of calcium oxalate.

Although these tailor-made additives were carefully designed, what we could not predict was the effect it would have on nucleation, growth, morphology, and phase transformation. As it has been stated many times in the literature, the effect of additives on crystal growth and morphology still remains a matter of mix and match. However, tailor-made additives cannot be discounted as effective method of controlling crystallization process when the right match has been determined.